Wings of Change: aPKC/FoxP-dependent plasticity in steering motor neurons underlies operant self-learning in *Drosophila*

Andreas Ehweiner[1], Carsten Duch[2] and Björn Brembs[1]*

1 Universität Regensburg, Institut für Zoologie - Neurogenetik, Regensburg, Germany.

2 Johannes Gutenberg Universität Mainz, Institute of Developmental Biology and Neurobiology (iDN), Mainz, Germany

* bjoern@brembs.net

Abstract

Motor learning is central to human existence such as in learning to speak or walk, sports moves or rehabilitation after injury. Evidence suggests that all forms of motor learning may share an evolutionary conserved molecular plasticity pathway. Here we present novel insights into the neural processes underlying a specific form of motor learning in the fruit fly *Drosophila*, operant self-learning. Our experiments suggest that for this type of motor learning, co-expression of atypical protein kinase C (aPKC) and the transcription factor *FoxP* is necessary in direct wing steering motoneurons. Some of these neurons are controlling wing beat amplitude when generating optomotor responses and we have discovered modulation of optomotor behavior after operant self-learning. Using CRISPR/Cas9 to knock out the canonical aPKC interaction partners *bazooka* and kidney and brain gene (KIBRA) in adult animals, we found that aPKC likely acts via non-canonical pathways in this form of learning. We also found that it takes more than a week before CRISPR/Cas9-mediated knockout of *FoxP* in adult animals impairs motor learning, suggesting that adult *FoxP* expression is required for operant self-learning.

1. Introduction

Motor learning is an essential component of human behavior and ubiquitous throughout the animal kingdom. The process of learning a motor skill can be influenced by a number of factors, such as the amount of training, the type of feedback, or the presence/absence of environmental cues. Regaining lost motor functions after brain or spinal cord injury is considered a crucial component of rehabilitation. Human language is acquired by a form of motor learning, and motor learning also appears to be a key invention that allowed the newly evolved animals in the Cambrian to become ambulatory (Keijzer et al., 2013; Arendt, 2021; Jékely, 2021). Vocal learning, such as learning to speak, is a form of motor learning (Walsh et al., 2006) that involves the Forkhead Box transcription factor family P (FoxP) in vertebrates (Lai et al., 2001; Zhang et al., 2002; Haesler et al., 2007; Fisher and Scharff, 2009; Takahashi et al., 2009; Bolhuis et al., 2010; Teramitsu et al., 2010; Scharff and Petri, 2011; French et al., 2012; Day et al., 2019; Co et al., 2020). Other, non-vocal forms of motor learning also involve FoxP genes in vertebrates (Groszer et al., 2008; Schreiweis et al., 2014; French et al., 2019; Lozano et al., 2021) and invertebrates (Mendoza et al., 2014). Vocal learn-

ing also shares the involvement of protein kinase C (PKC) with other forms of motor learning (Sakaguchi and Yamaguchi, 1997; Metzger and Kapfhammer, 2003; Rochefort et al., 2011; Colomb and Brembs, 2016; Gallimore et al., 2018), raising the possibility of a conserved motor learning pathway extending beyond these two components.

While motor learning shares various features with other forms of learning, such as operant learning producing habits or skill-learning, it is debated how many common biological mechanisms these different concepts share (Salmon and Butters, 1995; Krakauer et al., 2019; Du et al., 2022; Fresco et al., 2022). Understanding motor learning in a numerically smaller nervous system in a genetically tractable organism where one can not only study the motor learning process itself, but also its interactions with other forms of learning (Brembs, 2009), may help instruct these debates.

Here we provide further evidence about the specific manner in which FoxP and PKC are involved in a form of motor learning in the fruit fly *Drosophila*, operant self-learning at the torque meter. In this experiment, motor learning dissociates from other forms of learning such that genes involved in motor learning are not involved in other forms of learning and *vice versa* (Brembs and Plendl, 2008; Colomb and Brembs, 2010; Brembs, 2011). At the torque

meter, a fly is tethered between head and thorax such that it can move all other appendages. When beating its wings, the fly generates forces, some of which the torque meter can measure. Specifically, the torque meter measures torque around the vertical body axis, yaw torque (Götz, 1964). Even in the absence of any guiding cues, flies can learn to associate one torque domain (e.g., roughly corresponding to left or right, respectively, turning maneuvers) with a punishing heat beam (Wolf and Heisenberg, 1991). This experiment not only conceptually mimics other motor learning paradigms in that feedback is made immediately contingent on specific motor actions, but also via its dependence on *FoxP* and PKC genes (Mendoza et al., 2014; Colomb and Brembs, 2016). This form of motor learning has been termed operant self-learning to distinguish it from other forms of operant learning and to denote that the subject is learning about its own behavior, as opposed to some stimulus associated with the behavior (Colomb and Brembs, 2010).

For operant self-learning in *Drosophila*, it is not known in which neurons the *FoxP* gene is required and which PKC gene is involved. It is also unknown which pathway is engaged by PKC and whether FoxP expression is also re-

quired acutely in adult flies for this form of motor learning. In this work, we address all three research questions.

2. Materials and Methods

2.1. Strains and fly rearing

If not stated otherwise, flies were raised on standard cornmeal/molasses medium (Guo et al., 1996) at 25°C and 60% humidity at a 12-hour light/dark cycle. For experiments requiring the expression of temperature-sensitive Gal80, animals were raised at 18°C. To set up crosses for behavioral experiments, 20 females were placed together with five to eight males and were allowed to lay eggs for 24 hours. They were flipped daily into fresh vials, ensuring appropriate larval density. Flies were prepared the day before the experiment, allowing them time to recover. 24 to 48 hours old female flies were briefly immobilized using cold anesthesia. A thin triangular copper hook (0,05 mm diameter) was glued (3m Espe Sinfony, 3M Deutschland GmbH) between head and thorax, fixing both body parts to each other (Brembs, 2008). Each animal was kept individually in a small moist chamber with a few grains of sugar. For *tub-Gal80*^{ts} expression, animals were raised at 18°C and placed at 30°C for two days. Experiments were always performed at room temperature. For experiments using the gene-switch system, newly hatched

flies were placed on *Drosophila* instant medium (351.204, Schlüter Biologie, Eutin-Neudorf, Germany) containing the steroid hormone RU486 (200 µg/ml, CAS No.: 84371-65-3, Sigma-Aldrich, St. Louis, MO) for two days.

The UAS-g-KIBRA line was generated in the laboratory of Michael Krahn, Universität Münster. They cloned the following guide RNAs from KIBRA Intron-2: GTACTTACGACTGCTTCGAC and KIBRA Intron-4: GGGCACCGTGCAGATCAGCA in pCDF6 and inserted them in attP40.

156 **Table 1:** Fly strains used in this work.

Genotype	use	Bloomington	Flybase
;;nSyb-GS	driver	80699	FBti0201287
;;GMR55G08-GAL4	driver	50422	FBti0136906
;;GMR65A06-GAL4	driver	39330	FBti0137511
;;GMR20H05-GAL4	driver	47896	FBti0133817
;;ato-Gal4	driver		
ELAV-Gal4;;	driver		
ELAV-Gal4;Tub-Gal80ts;;	driver		
;;FoxP-iB-Gal4/TM3	driver		
;;FoxP-LexA	driver		
;;UAS-g-aPKC	effector	85862	FBti0210993
;;UAS-g-BAZ	effector	84234	FBti0207133
;;UAS-g-PKC53e	effector	76612	FBti0194968
;UAS-g-KIBRA	effector		
;;UAS-Cas9;	effector		
;;UAS-PKCi	effector	4589	FBti0010565
;;UAS-t:gRNA(4xFoxP)	effector		
;UAS-Cas9;;	effector		
C380-Gal4;;	driver	80580	FBti0016294
y[1] w[*]; Mi{Trojan GAL4.un} aPKC[MI10848-TG4.un]/SM6a	driver	77814	FBti0196316
LexAop-mD8-RFP-UAS-mCD8-GFP;TM3/TM6b	effector		
Wild type Berlin	wild type strain		

157 ## 2.2. Behavioral setups

158 Two different torque meters and setups
159 were used. Both torque meters were described

previously: The ‘Shiming’ meter (Tang and Juusola, 2010) and the ‘Götz’ meter (Götz, 1964)(RRID:SCR_017276), named after the authors. With flies attached to the torque meter via a clamp, both devices measure the rotational force (torque) around the animal’s vertical body axis. While the Götz meter is older than the Shiming meter, due to its rotational compensation it is technically more advanced and was included in a more modern version of the setup which was used in the later experiments, after the first data was collected using the Shiming setup. In both setups, the animal is surrounded by a cylindrical panorama (arena; diameter 58 mm), homogeneously illuminated from behind by either a projector (Götz: DLPLCR4500EVM, Texas Instruments) or a halogen lamp (Shiming: OSRAM 100W/12V), such that stationary flight in a controlled environment was achieved. An infrared laser (StockerYale Lasiris SNF series; 825 nm, 150 mW) was used as punishment in both setups. The laser was pointed from above onto the animal’s head, pulsed (approx. 200 ms pulse width ~4 Hz) and the intensity adjusted empirically for maximal heat avoidance and learning. The experiment is fully computer controlled, using custom software (Shiming: LabView, National Instruments, RRID:SCR_014325. Götz: DOI: 10.5281/zenodo.7102195).

2.3. Design of behavioral experiments

Before each self-learning experiment, the yaw torque range was adjusted using optomotor stimuli for each fly tethered to the torque meter. For the 'Shiming' setup, arena rotation for the optomotor stimulus was operated by hand. The direction of the rotation was reversed after the fly reached its asymptotic optomotor torque. During optomotor presentations before the self-learning experiment, the torque was adjusted to be zero-symmetric. This was to help facilitate unbiased torque preferences before training. Optomotor stimuli (15 vertical black stripes on a white background taking about 3.5s for a full rotation, i.e., a pattern wavelength of 24° at a pattern frequency of about 4.3 Hz) were presented for a duration of 30 s in each turning direction for flies in the 'Götz' setup. Because of this difference, experiments recorded with the Shiming device did not record optomotor periods such that their periods are numbered from 1 to 9 (Table 2), while optomotor periods for the Götz setup were included, such that the periods were numbered 1-17 (Table 3). Because we used four optomotor periods in the Götz setup, periods 5 to 13 are the periods in which self-learning was studied in this setup.

The main self-learning experiment then consisted of nine periods of two minutes duration. The laser was permanently off during the

first two periods, so that the fly could freely choose its direction of turning maneuvers without any feedback. In the following two training periods either the left or the right torque domain was associated with the punishing laser, without any hysteresis. The punished torque domain was alternated between experiments. The first two training periods were followed by one test period without punishment. Afterwards, the fly was trained again with the same side punished as before for another two 2-min. periods. Finally, no heat was applied in the final two test periods, allowing the fly to express its spontaneous yaw torque preference. Figures always show the preference in the first test period after the last training period, i.e., period 8 (performance index, PI8) in the Shiming setup and period 12 (PI12) in the Götz setup (Tables 2, 3). In the case where axis labels in the figures differ with regard to PI8 or PI12, these differences only indicate which setup was used. In all cases, the same first test period after the last training period was used to test for learning, irrespective of setup.

Table 2: Experimental sequence "Shiming Setup". All periods lasted 120s.

Period 1	**Period 2**	**Period 3**	**Period 4**	**Period 5**	**Period 6**	**Period 7**	**Period 8**	**Period 9**
Pretest	Pretest	Training	Training	Test	Training	Training	Test	Test
No heat	No heat	**Heat**	**Heat**	No heat	**Heat**	**Heat**	No heat	No heat

Table 3: Experimental sequence "Götz Setup". OM - optomotor. Torque learning periods (5-13) lasted 120s, while OM periods lasted 30s.

OM before				Experiment									OM after			
Period 1	Period 2	Period 3	Period 4	Period 5	Period 6	Period 7	Period 8	Period 9	Period 10	Period 11	Period 12	Period 13	Period 14	Period 15	Period 16	Period 17
OM	OM	OM	OM	Pretest	Pretest	Training	Training	Test	Training	Training	Test	Test	OM	OM	OM	OM
No heat	No heat	No heat	No heat	No heat	No heat	**Heat**	**Heat**	No heat	Heat	Heat	No heat	No heat	No heat	No heat	No heat	No heat

2.4. Data handling and statistical analysis of behavioral experiments

2.4.1. Data selection

To ensure proper punishment by the laser, each fly was exposed to the laser after the experiment, to ensure it was correctly adjusted. If the fly survived the laser for 15 seconds or more, the data were excluded from analysis. Data that did not show any or shifted optomotor responses, indicating either an unhealthy fly or an error with the measuring device, were also excluded. Data were also excluded if the fly did not experience the laser at least once during training. Lastly, flies with poor flight performance (constant stopping of flight) were also excluded from analysis. While these data were excluded from analysis, all complete traces are nevertheless included in

the published data sets, such that the inclusion criteria can be independently tested.

2.4.2. Data availability and analysis

The preference of a fly for right or left torque domain was quantified as the performance index $PI = (ta - tb)/(ta + tb)$. During training periods, tb indicates the time the fly is exposed to the heat and ta the time without heat. During tests, ta and tb refer to the times when the fly chose the formerly (or subsequently) unpunished or punished situation, respectively. Thus, a PI of 1 means the fly spent the entire period in the situation not associated with heat, whereas a PI of −1 indicates that the fly spent the entire period in the situation associated with heat. Accordingly, a PI of zero indicates that the fly distributed the time evenly between heated and non-heated situations and a PI of 0.5 indicates that 90 of the 120 s in that period were spent in the unpunished situation.

Analogously, optomotor (Table 3, OM) behavior was quantified by computing an OM asymmetry index. Straight lines or double sigmoidal models were fitted to individual torque traces from OM periods, depending on the detected slope of the optomotor response. From the fitted lines/models, optomotor magnitude was derived as either the intercept (lines) or the asymptote (double sigmoidal model). The

magnitude of left-turning torque was subtracted from the magnitude of right-turning torque and divided by the sum of both values. This results in an index that is zero for symmetric optomotor responses. The index becomes -1 for optomotor responses where clockwise ('right-turning') stimuli elicit no or left-turning torque (while counter-clockwise stimuli elicit left-turning torque). It becomes 1 for optomotor responses where counter-clockwise ('left-turning') stimuli elicit no or right-turning torque (while clockwise stimuli elicit right-turning torque). In brief, a positive optomotor asymmetry index indicates shifts away from symmetrical torque towards right-turning torque and a negative index indicates shifts towards left-turning torque.

All behavioral data are analyzed using R (R Project for Statistical Computing) (RRID:SCR_001905). The collection of R-scripts evaluating the time series data can be found at DOI 10.5281/zenodo.10041052. The data model pertaining to the XML raw data files and the YAML data set files can be found at 10.5281/zenodo.7101734. In brief, the XML data files contain both the meta-data for each single fly experiment as well as the time series data covering the entire experiment. The single YAML file per dataset contains the experimental design, such as which data files belong

to which experimental group, the kind of statistics to be performed, significance levels used, experimenter comments and data inclusion/exclusion. The main R-Script reads the YAML dataset files and performs the appropriate computations for quality control, analysis and statistics.

Quality control is performed on each single fly XML file and included in the published data sets. Each single fly experiment XML file is thus accompanied by a single fly HTML quality control report sheet containing both plots of the raw time series data as well as a number of evaluations necessary to assess the proper execution of the experiment and the quality of the resulting data.

Data analysis and statistics for each dataset are reported in an HTML dataset evaluation sheet. A complete dataset thus consists of one XML raw data file and one HTML quality control sheet for each fly, plus a single YAML dataset file and one HTML dataset evaluation sheet.

The datasets were published using a custom Python script (DOI: 10.5281/zenodo.7101741) that synchronizes the collected data on the local computer with the University of Regensburg publication server. Persistent identifiers for each dataset are listed in the figure legends.

2.4.3. Statistics

PIs are statistically evaluated in two complementary ways, using both frequentist and Bayesian statistics. Following previous studies (Liu et al., 1999, 2006; Brembs and Hempel de Ibarra, 2006; Brembs and Wiener, 2006; Brembs and Plendl, 2008; Brembs, 2009), individual PIs of the first test after the last training period are tested against zero to evaluate the ability of the manipulated flies to show a preference towards the unpunished torque domain. We used a Wilcoxon test in the frequentist case and computed a Bayes Factor for the Bayesian version. We set the alpha value for the Wilcoxon test at 0.5% as suggested by (Benjamin et al., 2018), such that p-values below 0.005 and Bayes factors above 5 for the same group of flies would be considered compelling evidence that the flies were able to learn. Conversely, Bayes Factors below one together with p-values higher than 0.05 were considered evidence that the flies were not able to show self-learning. Finally, groups where the two statistics were in conflict or intermediate, were considered inconclusive. Thus, both the Bayesian and the frequentist criteria had to be met in order to claim that a genetic manipulation interfered with operant self-learning.

2.5. Gene expression analysis in flight steering motor neuron terminals

2.5.1. Dissection

The axon terminals on flight steering muscles were tested immunocytochemically for the expression of *FoxP* and aPKC in flies expressing LexAop RFP under the control of FoxP-Lex and UAS td-GFP under the control of aPKC-trojan GAL4 (LexAop RFP, UAS td-GFP / aPKC-Trojan-GAL4; FoxP-LexA / +). In addition, synapses at neuromuscular junctions were labeled with the active zone marker *bruchpilot* (*brp*, (Kittel et al., 2006)). Animals were dissected in normal saline along the dorsal midline and bent open with minute pins inserted through the dorsalmost edge of the dorsal longitudinal flight muscles (DLMs). The heart, gut, fat tissue, and other connective tissue were removed to expose the ventral nerve cord (VNC) and the musculature. Next, on both sides the DLMs and dorsoventral flight muscles (DVMs) were carefully removed layer by layer to expose the direct flight steering muscles, which are located close to the lateral cuticle of the thorax. Preparations were rinsed 5-10 times in saline to remove debris from the dissection procedure, and specimens were fixed for 1h in 4% paraformaldehyde in 0.1 M PBS buffer at room temperature (22°C). After fixation specimen paraformaldehyde was exchanged by 0.1 M PBS buffer.

2.5.2. Immunohistochemistry of motor terminals

Following fixation, specimens were washed 6 x 20 min in 0.1 M PBS buffer at room temperature. Next, preparations were washed 3 x 1 h in 0.1 M PBS-Tx (0.3%) buffer at room temperature and incubated with primary antibodies (mouse α-brp, 1:500 (Hybridoma bank, NC82)); chicken α-GFP (1:1000, Life Technologies A10262), and rabbit α-mCherry, (1:500, PAS-34974)) in 0.1 M PBS-Tx (0.3%) buffer at 4°C for 24 to 36 hs. Following primary antibody incubation, preparations were washed 6 x 1 h in 0.1 M PBS buffer at room temperature. Next animals were incubated in secondary antibodies: donkey α-mouse Alexa 647 (JacksonImmunoResearch 715-605-150), donkey α-chicken Alexa 488 (Dianova 703-545-155), and donkey α-rabbit Alexa 568 (Invitrogen A10042) in 0.1 M PBS-Tx (0.15%) buffer at 4°C for 24 to 36 hs. Following secondary antibody incubation, preparations were washed 3 x 1 h in 0.1 M PBS buffer at room temperature, dehydrated in an ascending ethanol series (50, 70, 90, and 2 x 100 % EtOH, 15 minutes each), and cleared for 5 min in methyl salicylate. Finally, preparations were mounted in methyl salicylate in between two coverslips that were glued onto both sides of a round hole (10 mm diameter) drilled into custom made metal slides of 188 µm thickness (Vonhoff et al., 2013). Briefly, one cover slip was fixated with superglue underneath the hole,

the space was filled with methyl salicylate, the preparation transferred into the mounting media, and another coverslip was carefully placed on top of the hole, so that no air remained in the methyl salicylate filled hole. The top coverslip was fixed to the metal slide with transparent nail polish (DM Markt, Mainz, Germany). After 20 minutes to let the nail polish dry the preparation was transferred to the microscope. In total 11 animals were subjected to immunocytochemistry on direct flight muscles. In 9 of these 11 preparations, we were able to identify only subsets of the direct wing steering muscles under investigation. These subsets yielded identical results with respect to aPKC and FoxP expression as the two preparations with complete sets of direct muscles as shown in figure 3.

2.5.3. Confocal laser scanning microscopy

Preparations were scanned with a Leica (Leica Microsystems, Germany) SP8 confocal laser scanning microscope (CLSM) under either a 20x oil (NA = 0.75) or a 40x oil (NA = 1.3) lens at an image format of 1024 times 1024 pixels. Z-step size was 2 µm for the 20x lens (resulting in voxel dimensions of 0.57 x 0.57 x 2 µm) and 1 µm for the 40x lens (resulting in voxel dimensions of 0.28 x 0.28 x 1 µm). Alexa 488 was excited with an argon laser at 488 nm and detected with a photomultiplier between 495 and 530 nm wavelength. Alexa 488 was excited

with a solid state laser at 561 nm and detected with a photomultiplier between 570 and 610 nm wavelength. Alexa 647 was excited with a red helium neon laser at 633 nm and detected with a photomultiplier between 640 and 670 nm wavelength. All image stacks were stored as .lei files and further analyzed with Las X software (Leica Microsystems, Germany). Selected fields of view were used for maximum intensity projection views, which were exported as 24 bit three color tiff images and further processed with Corel Draw 11.

2.5.4. Data availability

Confocal image stacks can be found at: 10.5281/zenodo.10021110

3. Results

3.1. Self-learning requires a*PKC* in *FoxP* motor neurons

Colomb and Brembs (2016) discovered that blocking all protein kinase C (PKC) isoforms in neurons using the inhibitory peptide PKCi abolished operant self-learning. We replicated their results by expressing PKCi pan-neuronally. In one group, PKCi was expressed both during development and in the adult flies. In the other group, PKCi expression was restricted to adulthood only, by using the temperature-sensitive Gal4 inhibitor *tub-Gal80*^{ts} (see methods for details). Temporally unrestricted pan-neural expression did not impair

self-learning, while expression restricted to neurons in adult flies abolished self-learning (Fig. 1A). This result may seem surprising, but compensation for experimental manipulations of PKC activity through development has been reported numerous times in the literature (Tsokas et al., 2016; Sacktor and Hell, 2017; Trzesniewski et al., 2019; Hiroki and Iino, 2022; Teegala et al., 2022) and conforms with our own unpublished observations using PKCi. Thus, the important result here is that short-enough (to escape compensation) expression of PKCi in adult neurons impairs operant self-learning. Expressing PKCi only in cells expressing isoform B of the FoxP gene also abolished self-learning, even without temporal control, suggesting that PKC activity is required in FoxP-positive neurons.

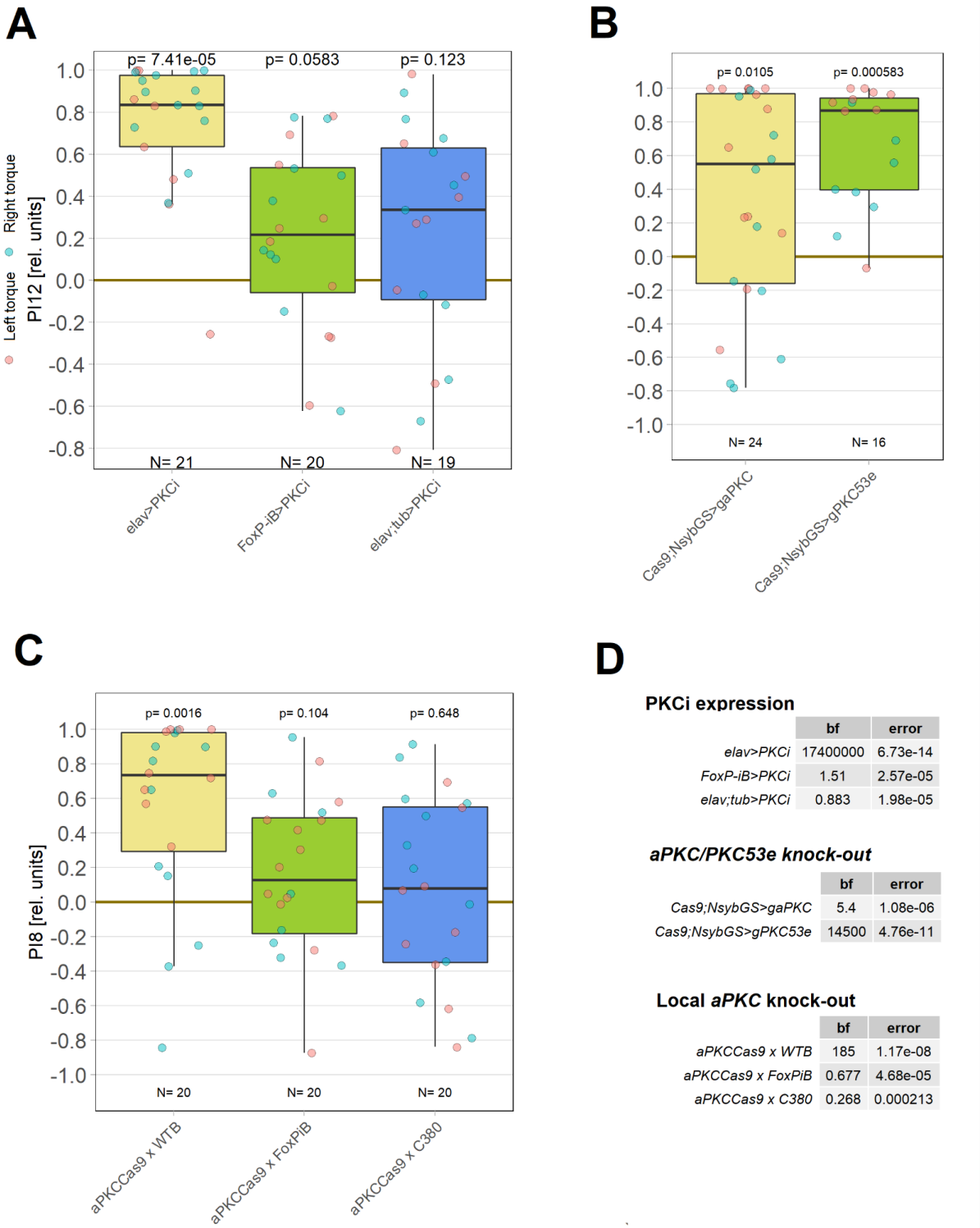

PKCi expression

	bf	error
elav>PKCi	17400000	6.73e-14
FoxP-iB>PKCi	1.51	2.57e-05
elav;tub>PKCi	0.883	1.98e-05

aPKC/PKC53e knock-out

	bf	error
Cas9;NsybGS>gaPKC	5.4	1.08e-06
Cas9;NsybGS>gPKC53e	14500	4.76e-11

Local *aPKC* knock-out

	bf	error
aPKCCas9 x WTB	185	1.17e-08
aPKCCas9 x FoxPiB	0.677	4.68e-05
aPKCCas9 x C380	0.268	0.000213

Figure 1: For operant self-learning, *aPKC* is required in motor neurons.

Plotted are performance indices for the first period after training (PI8/PI12). Each colored dot represents a single fly experiment. Red dots denote experiments where the fly was punished on its left turning torque domain, blue dots denote flies that were punished on their right turning domain. Box plots denote medians, quartiles and non-outlier range. Statistical analyses test for differences of PIs against zero.

A. Inhibiting all protein kinase C isoforms with the inhibitory peptide PKCi. Constitutive, pan-neuronal expression PKCi (left, yellow), leads to high PIs and a large Bayes Factor, indicating this manipulation left self-learning intact. Expressing PKCi either in FoxP-isoform B positive neurons without temporal

control (middle, green), or in all neurons but restricted to adulthood using *tub-Gal80*^{ts} (right, blue, see methods for detail) yields low PIs, high p-values and low Bayes factors, indicating self-learning is impaired. Data: 10.5283/epub.52958

B. Pan-neuronal knock-out of two different PKC genes with CRISPR/Cas9 in adulthood (using the GeneSwitch system and feeding RU486 to adult flies, see methods for details) suggests aPKC is necessary for operant self-learning. Knocking out atypical PKC (yellow, left) yields moderate PIs, p-values and Bayes factors, indicating some effect on operant self-learning, while the high PIs, low p-values and high Bayes factor of the group where PKC53E was knocked out (right, green) indicate their self-learning is intact. Data: 10.5283/epub.52957

C. Knocking out aPKC in motor neurons or *FoxP*-neurons impairs operant self-learning. Expressing the CRISPR/Cas9 components either in *FoxP* isoform B-positive neurons (green, middle) or in motor neurons (blue, right) leads to low PIs, high p-values and low Bayes Factors, indicating their self-learning is strongly impaired. Control flies with only the CRISPR/Cas9 genetic elements but no driver, show high PIs, a low p-value and a high Bayes Factor, indicating their self-learning is intact. Data: 10.5283/epub.52944

D. Bayesian statistics for the three datasets.

Colomb and Brembs (2016) also discovered that restricting PKCi expression to motoneurons (MNs) was sufficient to impair self-learning. To help determine which PKC may be involved in the mechanism, we screened RNA-Seq databases for PKC genes expressed in MNs. Restricting candidates to those where gRNA lines were available for CRISPR/Cas9-mediated gene knock-out yielded only two genes: the atypical PKC (aPKC) and the diacylglycerol-activated PKC53E. Knocking out each gene pan-neuronally in adult flies and testing the manipulated animals for operant self-learning showed excellent learning performance in the PKC53E-manipulated flies (Fig. 1B), clearly ruling out PKC53E as the gene involved in operant self-learning. The performance of the aPKC-manipulated flies was inconclusive: their preference scores were somewhat lower, not reaching our criteria for significant learning,

but at the same time too high to be confident in the result (Fig. 1B).

As PKC activity is required in MNs (Colomb and Brembs, 2016), we limited the aPKC knock-out to these neurons and this abolished self-learning (Fig. 1C). Testing the hypothesis articulated above that aPKC activity is required in FoxP neurons, we also knocked out aPKC in FoxP neurons, which also abolished self-learning. (Fig. 1C).

3.2. *aPKC* and *FoxP* are co-expressed in identified flight steering MNs

The behavioral data presented above thus support the hypothesis that the plasticity mediating operant self-learning takes place in neurons that co-express both *FoxP* and *aPKC*. Whole-mount confocal microscopy of fly central nervous systems with *aPKC*-Gal4 and *Foxp*-LexA expression suggest that neurons expressing both *aPKC* and *FoxP* exist only in the ventral nerve cord (VNC, Fig. 2A, B). We identified co-expressing neurons in all neuromers of the VNC, with the ventral location of the mesothoracic *aPKC/FoxP* neurons suggesting potential wing MNs (Fig. 2C)(Phelps et al., 2021). To ascertain the identity of this ventral cluster of co-expressing neurons, we marked MNs with the driver line D42-Gal4 and used FoxP-LexA to stain all *FoxP* neurons. With these labels, we identified a ventral sub-population of putative

wing MNs expressing *FoxP*, which match the location of the *aPKC/FoxP* neurons identified before (Fig. 2D). Both the C380 driver used in Fig. 1 and the D42 driver used here, label not only MNs but also other neurons, in particular cholinergic neurons. However, the lines overlap in MNs in the VNC. *FoxP* is also expressed in these MNs and knocking out aPKC in these neurons also impaired operant self-learning. While each line of evidence is suggestive, at best, together, these lines of evidence converge on the hypothesis that wing steering MNs expressing both aPKC and FoxP may be important for operant self-learning.

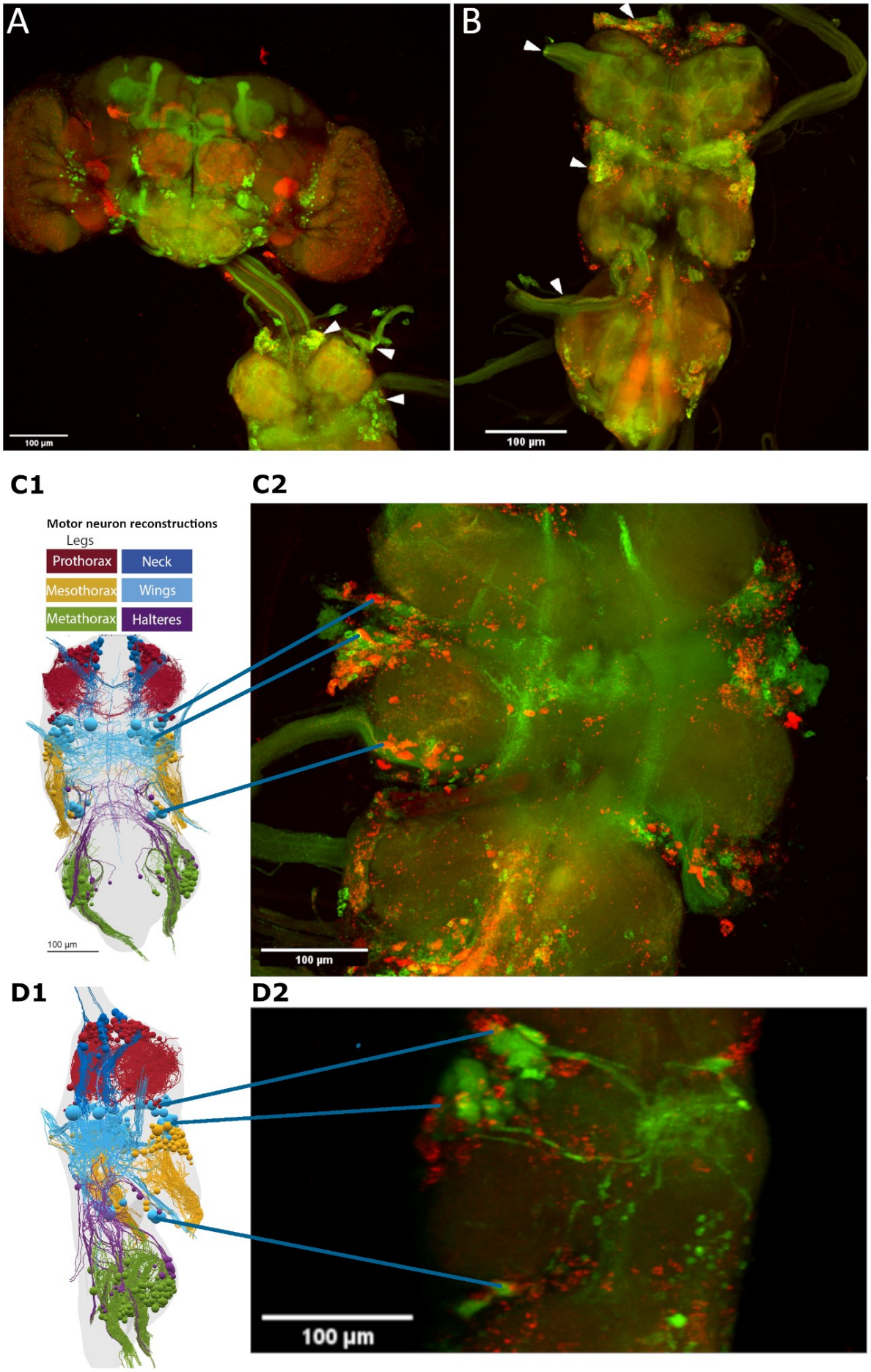
A
B
100 µm
100 µm
C1
C2
Motor neuron reconstructions
Legs
Prothorax
Neck
Mesothorax
Wings
Metathorax
Halteres
100 µm
100 µm
D1
D2
100 µm

Figure 2: FoxP and aPKC are coexpressed in MNs.

Confocal stacks of whole mount preparations of central nervous systems; A-C: green - aPKC-Gal4>CD8::GFP, red - FoxP-LexA>CD8::RFP; D: green - D42-Gal4>CD8::GFP, red - FoxP-LexA>CD8::RFP. Confocal image stacks available at:

A. Adult brain (top) with ventral nerve cord (VNC, bottom) attached. No co-expressing cells can be observed in the brain, while such neurons(yellow) are readily observable in all neuromers of the VNC (arrowheads).

B. VNC with *aPKC/Foxp* coexpression (yellow) both in cell bodies and fiber tracts in nerves (arrowheads).

C. C1: Dorsal view of motor neuron reconstruction (modified from (Phelps et al., 2021). C2: Confocal image stack of dorsal view of the mesothoracic neuromer with putative wing MNs expressing both *aPKC* (green) and *FoxP* (red) marked.

D. D1: Lateral view of motor neuron reconstruction (modified from (Phelps et al., 2021). D2: Confocal image stack of mesothoracic neuromer with all MNs (green) and FoxP neurons (red) marked. This lateral view supports the hypothesis that the ventral cluster of *aPKC/FoxP* neurons indeed comprises wing MNs.

These results, together with the recently published draft VNC connectome (Azevedo et al., 2022), prompted us to analyze the direct wing steering muscles for innervation by MNs with both aPKC and *FoxP* expression. Each direct steering muscle is innervated by one single identified MN (Trimarchi and Schneiderman, 1994). Thus, identifying the muscles reveals the identity of the corresponding MNs. To test for the expression of aPKC and *FoxP* in MNs that innervate direct wing muscles, we expressed UAS-GFP under the control of aPKC-Gal4 (Fig. 3, second column) and RFP under the control of FoxP-lexA (Fig. 3, third column). The signal of each fluorescent reporter was further enhanced by immunocytochemistry, and the active zone marker *bruchpilot* (*brp*; (Kittel et al., 2006) was used to label the neuromuscular synapses in flight MN axon terminals (Fig. 3, fourth column). In total, *Drosophila* is equipped with 12 flight steering muscles each of which likely contributes to a distinct function in flight

control (Whitehead et al., 2022). The activation patterns of four of these muscles have been analyzed in response to optomotor stimulation during flight (first and second basalar muscles b1 and b2, as well as first pterale I muscle (i1) and the third pterale II muscle (iii1) (Heide and Götz, 1996; Dickinson and Tu, 1997; Whitehead et al., 2022). A schematic of these 4 direct flight muscles plus five adjacent ones that were analyzed in this study illustrates their spatial arrangement, shapes, and depicts which ones are innervated by steering MNs that express both aPKC (green) and FoxP (magenta), only one of both, or neither of them (grey; Fig. 3A1).

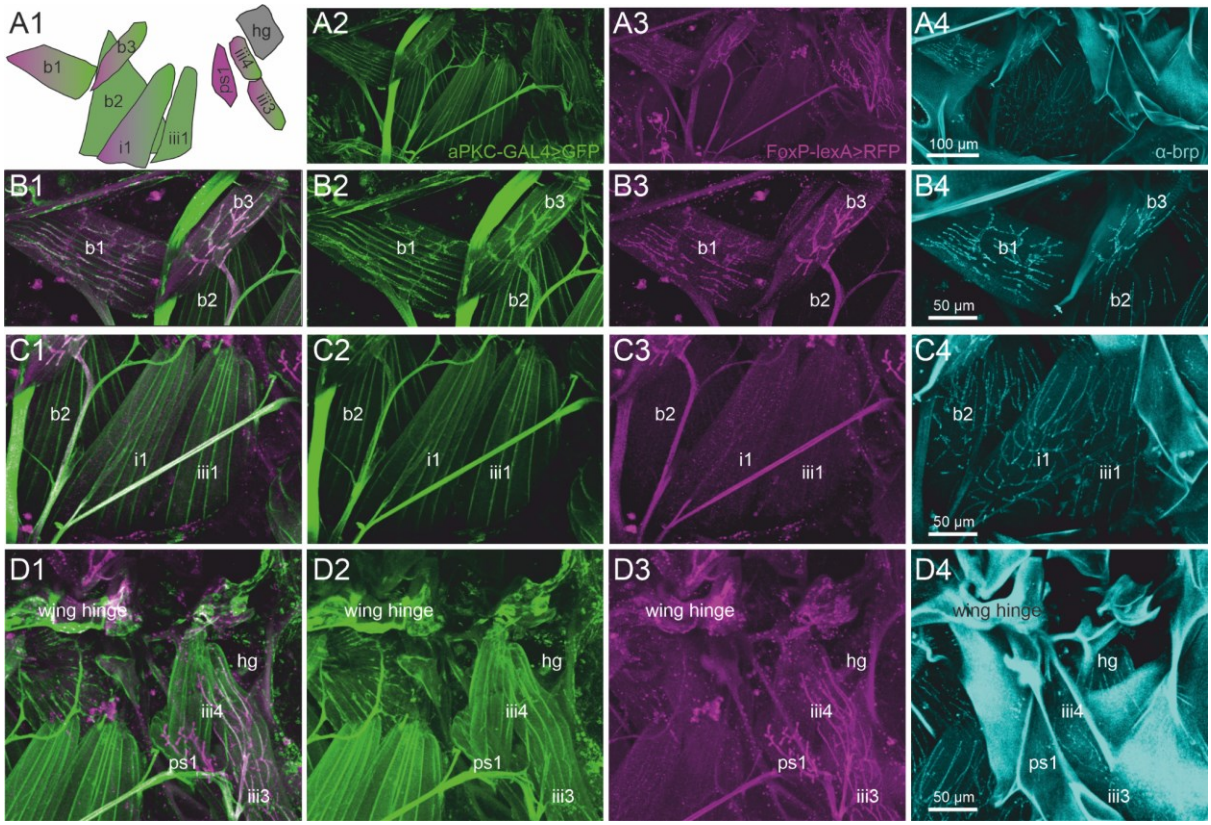

Figure 3. A subset of direct wing muscles is innervated by FoxP/aPKC co-expressing MNs.

Representative projection view of MN terminals on the direct flight steering muscles in animals with GFP label in aPKC expressing cells (aPKC-Gal4>CD8::GFP, green), RFP expression in FoxP expressing cells (FoxP-LexA>CD8::RFP, magenta), and immunolabel for the presynaptic active zone marker *bruchpilot* (*brp*, cyan) reveal which direct flight steering MNs express either aPKC, or FoxP, or both, or none of both but only *brp* in presynaptic active zones. **(A1)** depicts the orientation, shape, and abbreviated names of direct flight steering muscles and summarizes which ones are innervated by aPKC expressing MNs (green), by FoxP expressing MNs (magenta), or by MNs without FoxP and aPKC expression (grey). **(A2)** Projection view of direct flight muscles and their innervation with GFP expression under the control of aPKC-GAL4 (green) at 20x magnification. **(A3)** Same preparation, image stack, and field of view but with RFP expression under the control of FoxP-lexA (magenta). **(A4)** Same preparation, image stack, and field of view with *brp* immunolabel (cyan) in presynaptic active zones of flight steering MNs. **(B1-B4).** Same preparation but with selective enlargement of the 3 basalare muscles (b1-b3), with all 3 labels in **(B1)**, GFP label in aPKC expressing cells (green, **B2)**, RFP label in FoxP expressing cells (magenta, **B3)**, and Brp label in presynaptic active zones (cyan, **B4)**. Muscles b1 and b3 are innervated by steering MNs with aPKC and FoxP expression, but b2 is devoid of FoxP expressing innervation. **(C1-C4)** Same preparation but with selective enlargement of second basalare (b2) and the adjacent pterale 1 (i1) and pterale II (iii3) muscles with all 3 labels **(C1)**, GFP label in aPKC expressing cells (green, **C2)**, RFP label in FoxP expressing cells (magenta, **C3)**, and *brp* label in presynaptic active zones (cyan, **C4)**. Only i1 is faintly labeled for terminals with aPKC FoxP expression. **(D1-D4)** Same preparation but with selective enlargement of the pterale II muscles iii3 and iii4, the adjacent pleurosternal muscle (ps1), and the posterior notal wing process muscles (hg) muscles with all 3 labels **(D1)**, GFP label in aPKC expressing cells (green, **D2)**, RFP label in FoxP expressing cells (magenta, **D3)**, and Brp label in presynaptic active zones (cyan, **C4)**. The pterale II muscles iii3 and iii4 are innervated by terminals with aPKC and FoxP expression.

Representative maximum intensities projection views at 20x magnification allow us to visualize all nine flight steering muscles investigated in one field of view (Figs. 3A2-A4). Except the pleurosternal muscle 1 (ps1) and the posterior notal wing process muscles (hg), all other steering muscles are innervated by aPKC-positive MNs (Figs. 3A1, A2, green). By contrast, six of the nine steering muscles are innervated by *FoxP*-positive MNs, including the basalars b1 and b3, the pterale i1, iii3, and iii4, as well as the pleurosternal muscle ps1 (Figs. 3A1, A3, magenta). A subset of five flight steering muscles is innervated by MNs that express both genes that are required for operant self-learning. These are b1, b3, i1, iii3, and iii4 (Fig. 3A).

Selective enlargements at 40x magnification were used to better visualize the axon terminals on those steering muscles of particular interest, with figure 3 panels B1-B4 focussing on the three muscles that insert at the basalar sclerite, and are thus named basalar 1-3 (b1-b3). Prominent labels of both aPKC (green) and *FoxP* (magenta) are present on axon terminals of the steering muscles b1 and b3, but the motor axon innervating b2 is devoid of *FoxP* signal (Fig. 3, B1-B4).

Muscle b1 has been reported to fire once every wingbeat (Heide and Götz, 1996) during straight flight, during the transition

from up- to downstroke. Optomotor stimulation causes phase shifts of b1 firing in the wing beat cycle, which in turn cause changes in wing beat amplitude both in the fruit fly *Drosophila* (Heide and Götz, 1996) as well as in the blowfly, *Calliphora* (Tu and Dickinson, 1996). The activity of b3 during flight has not been recorded electrophysiologically, but the muscle exhibits very similar morphological properties compared to b1. Both b1 and b3 are orientated similarly relative to the body axis and the wing hinge, and both are innervated by MNs with particularly large diameter axons (Figs. 3B1-B3) and particularly large active zones (Fig. 3B4), suggesting similar functional roles. Steering muscle b2 is also innervated by large diameter axons (Fig. 3C1) with large presynaptic active zones (Fig. 3C4). However, aPKC expression is detected along the motor axon but not in the axon terminals (Figs. 3C1, C2, C4), and the motor axon is devoid of *FoxP* (Fig. 3C3). Although b2 has been reported to respond to optomotor stimulation, its phasic bursting responses correlate with rapid changes in wing beat amplitude as observed during body saccades (Heide and Götz, 1996).

Figure 3 panels C1-C4 move the field of view posteriorly and show the pterale 1 muscle i1 and the pterale 2 muscle iii1. Muscle i1 is innervated by a MN with faint aPKC (Fig. 3C2) and faint *FoxP* (Fig. 3C3) expression along the axon

but not in axon terminals. i1 has been reported to respond to optomotor stimulation, but its specific role in optomotor control remains largely unknown (Heide and Götz, 1996). Steering muscle iii1 shows some faint aPKC signal (Fig. 3C2) but is devoid of any *FoxP* label (Fig. 3C3) and does not participate in optomotor flight control (Heide and Götz, 1996).

The roles in flight control of the remaining four steering muscles (ps1, iii3, iii4, and hg; Figs. 3D1-D4) in *Drosophila* are not fully understood. However, iii3 and iii4 are innervated by MNs with aPKC (Fig. 3D2) and *FoxP* (Fig. 3D3) expression. Axon terminals on ps1 are *FoxP* positive (Fig. 3D3) but lack any aPKC label (Fig. 3D2). Active zones on steering muscle hg are visible through the *brp* label (Fig. 3D4) but the motor axon on hg is devoid of both aPKC (Fig. 3D2) and *FoxP* (Fig. 3D3).

3.3. Self-learning breaks optomotor symmetry

Because it is not known at which torque meter reading the fly actually generates zero angular momentum, before each torque learning experiment, it is crucial to set the average of the asymptotic left and right optomotor response magnitudes to zero (Fig. 4A1, see Materials and Methods for details). This is to avoid an initial bias in the torque preference before training and with the assumption that the midpoint between the maximal optomotor responses roughly corresponds to flying straight

(i.e, zero angular momentum). During the ensuing conditioning procedure, flies show spontaneous torque fluctuations that can reach or even exceed the ones elicited by optomotor stimulation in magnitude. Within each torque domain (i.e., 'left' or 'right', respectively), the temporal patterns (i.e., slow or fast) of torque fluctuations and their relative direction (i.e., more or less torque) are irrelevant for the heat stimulus as long as the zero point is not crossed: heat remains either on or off until the fly switches torque domains. At times, the appearance of these spontaneous torque fluctuations can mimic those elicited during optomotor stimulation. Therefore, the described role of the steering MNs co-expressing aPKC and FoxP (Fig. 3) in large torque fluctuations elicited by optomotor stimuli prompted the hypothesis that optomotor behavior should be affected by our operant conditioning if the training affects the same motor neurons that control both elicited and spontaneous torque fluctuations.

To test this hypothesis, we analyzed the optomotor responses after training of a cohort of wild type Berlin flies (Fig. 4B; control flies from a separate research project). We found that the asymptotic magnitude of the optomotor response on the punished side was reduced after operant training, while the optomotor response on the unpunished side remained unaltered compared to before training

(Fig. 4B1). Quantifying this observation revealed a significant difference in the optomotor asymmetry after training (Fig. 4B2) but not before training (Fig. 4A2) between the two experimental groups.

Before Training

A1

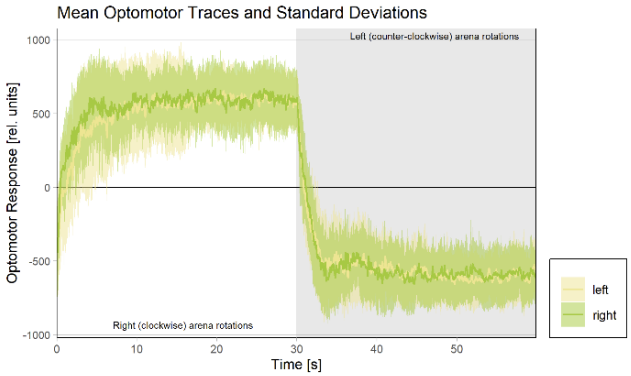

A2

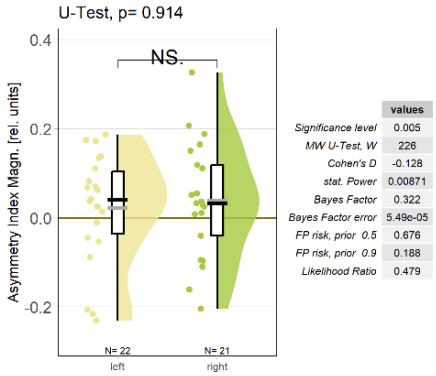

	values
Significance level	0.005
MW U-Test, W	226
Cohen's D	-0.128
stat. Power	0.00871
Bayes Factor	0.322
Bayes Factor error	5.49e-05
FP risk, prior 0.5	0.676
FP risk, prior 0.9	0.188
Likelihood Ratio	0.479

A3

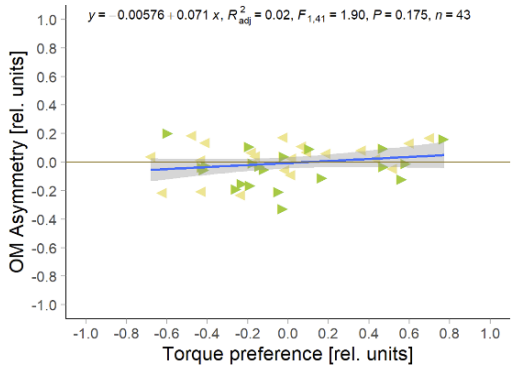

A4

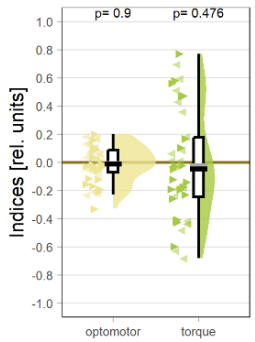

After Training

B1

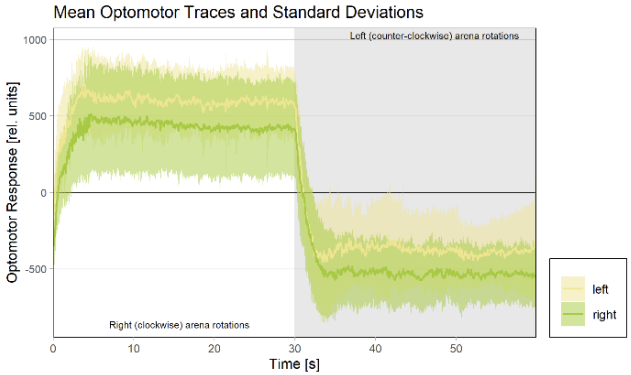

B2

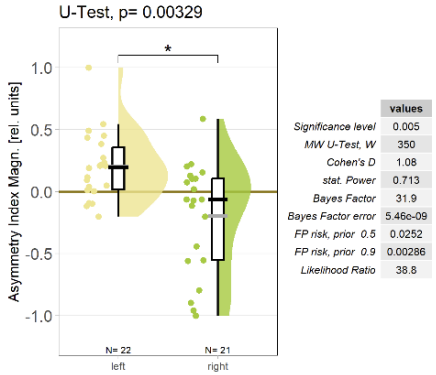

	values
Significance level	0.005
MW U-Test, W	350
Cohen's D	1.08
stat. Power	0.713
Bayes Factor	31.9
Bayes Factor error	5.46e-09
FP risk, prior 0.5	0.0252
FP risk, prior 0.9	0.00286
Likelihood Ratio	38.8

B3

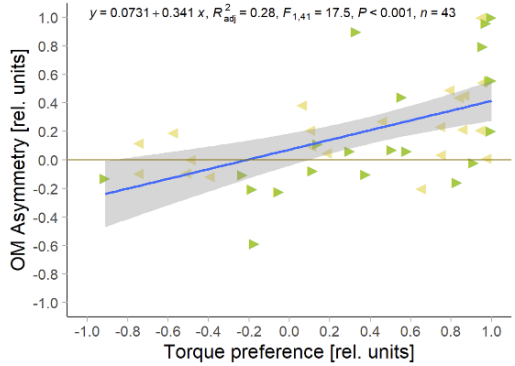

B4

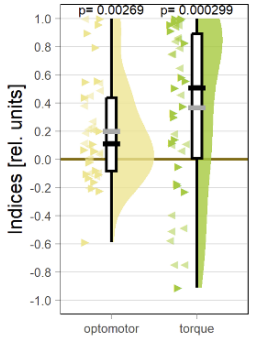

Fig. 4. Associating one torque domain with heat changes optomotor behavior.

A. Measurements before training

A1 Averaged optomotor traces of flies punished either on the 'left'(yellow) or on the 'right' (green) torque domain. Both groups show similar response magnitudes in either direction of the optomotor stimulus.

A2 Optomotor asymmetry indices for flies punished either on the 'left'(yellow) or on the 'right' (green) torque domain. The values for both groups spread around zero. Positive values indicate a shift towards positive (right-turning) torque. Both frequentist and Bayesian analyses are displayed to the right of the plots and indicate no difference between the groups.

A3 Regression analysis between torque preference and optomotor asymmetry. Optomotor values were adjusted such that positive values indicate a shift towards the unpunished torque domain. No significant correlation was observed. Left-pointing arrowheads (yellow) denote flies punished on left-turning torque and right-pointing arrowheads (green) denote flies punished on right-turning torque.

A4 Comparison of optomotor asymmetry (left, yellow) and torque preference(right, green) indices. Here again, optomotor values were adjusted such that positive values indicate a shift towards the unpunished torque domain. Both measures vary around the zero point and Wilcoxon tests against zero are not significant (p-values above each plot). Left- and right-pointing arrowheads denote punishment directions as before.

B. Measurements after training

B1 Averaged optomotor traces of flies punished either on the 'left'(yellow) or on the 'right' (green) torque domain. A reduction of the optomotor response magnitude on the punished, but not on the unpunished side can be observed.

B2 Optomotor asymmetry indices for flies punished either on the 'left'(yellow) or on the 'right' (green) torque domain. Positive values indicate a shift towards positive (right-turning) torque. The values for each group have now shifted towards the unpunished side compared to the values before training. Both frequentist and Bayesian analyses are displayed to the right of the plots and indicate a significant difference between the groups.

B3 Regression analysis between torque preference and optomotor asymmetry. Optomotor values were adjusted such that positive values indicate a shift towards the unpunished torque domain. A significantly positive correlation was observed, such that higher torque preferences entailed a larger optomotor asymmetry. Left-pointing arrowheads (yellow) denote flies punished on left-turning torque and right-pointing arrowheads (green) denote flies punished on right-turning torque.

B4 Comparison of optomotor asymmetry (left, yellow) and torque preference(right, green) indices. Here again, optomotor values were adjusted such that positive values indicate a shift towards the unpunished torque domain. Both measures are shifted towards more positive values and Wilcoxon tests against zero are now significant for both variables (p-values above each plot). Left- and right-pointing arrowheads denote punishment directions as before.

Data available at: 10.5283/epub.54804

An important question with regard to the functional significance of this change in optomotor asymmetry is whether the amount of torque preference after training reflects the amount of optomotor asymmetry. There is no significant correlation between torque prefer-

ence and optomotor asymmetry before training (Fig. 4A3; as expected as the optomotor response was adjusted to be as symmetrical as practically possible). Once the flies have completed the training phase, torque preference becomes a significant predictor of optomotor asymmetry (Fig. 4B3). These results corroborate our hypothesis that the wing MNs identified above, specifically those that have been shown to be involved in generating optomotor responses (Heide and Götz, 1996; Whitehead et al., 2022), constitute a site of the plasticity mediating operant self-learning in *Drosophila*. We also tested whether it would be sufficient to test for optomotor asymmetry after training as a proxy measure for torque preference. Before training, as expected, both measures showed similar values ranging around the zero point (Fig. 4A4). After training, both measures did deviate from zero towards the unpunished direction, but the effect was noticeably larger for torque preference than for optomotor asymmetry (Fig. 4B4). Together with the correlation explaining about a third of the variance (Fig. 4B3), these data may indicate that the MNs are an important, but not the only site of plasticity in this form of learning.

3.4. Spatial genome editing: *FoxP* likely not required in the brain

Optomotor analysis (Fig. 4) suggests there may be additional sites of plasticity besides wing steering MNs. *FoxP*-positive neurons in the brain are straightforward potential candidates for such additional sites. We therefore performed spatial CRISPR/Cas9-based genome editing without restricting the manipulation to the adult stage. At the time when these experiments were performed, no driver lines with *FoxP*-overlapping expression in the Saddle and Vest regions were available. Therefore, we tested driver lines expressing in the protocerebral bridge (PCB, Fig. 5A), the PCB and adjacent central complex neuropils (see Materials and Methods for details, Fig. 5B) and the dorsal cluster neurons (Fig. 5C). No self-learning impairment was observed following *FoxP* knockout in these brain areas, suggesting that *FoxP* expression is not necessary in these areas for operant self-learning.

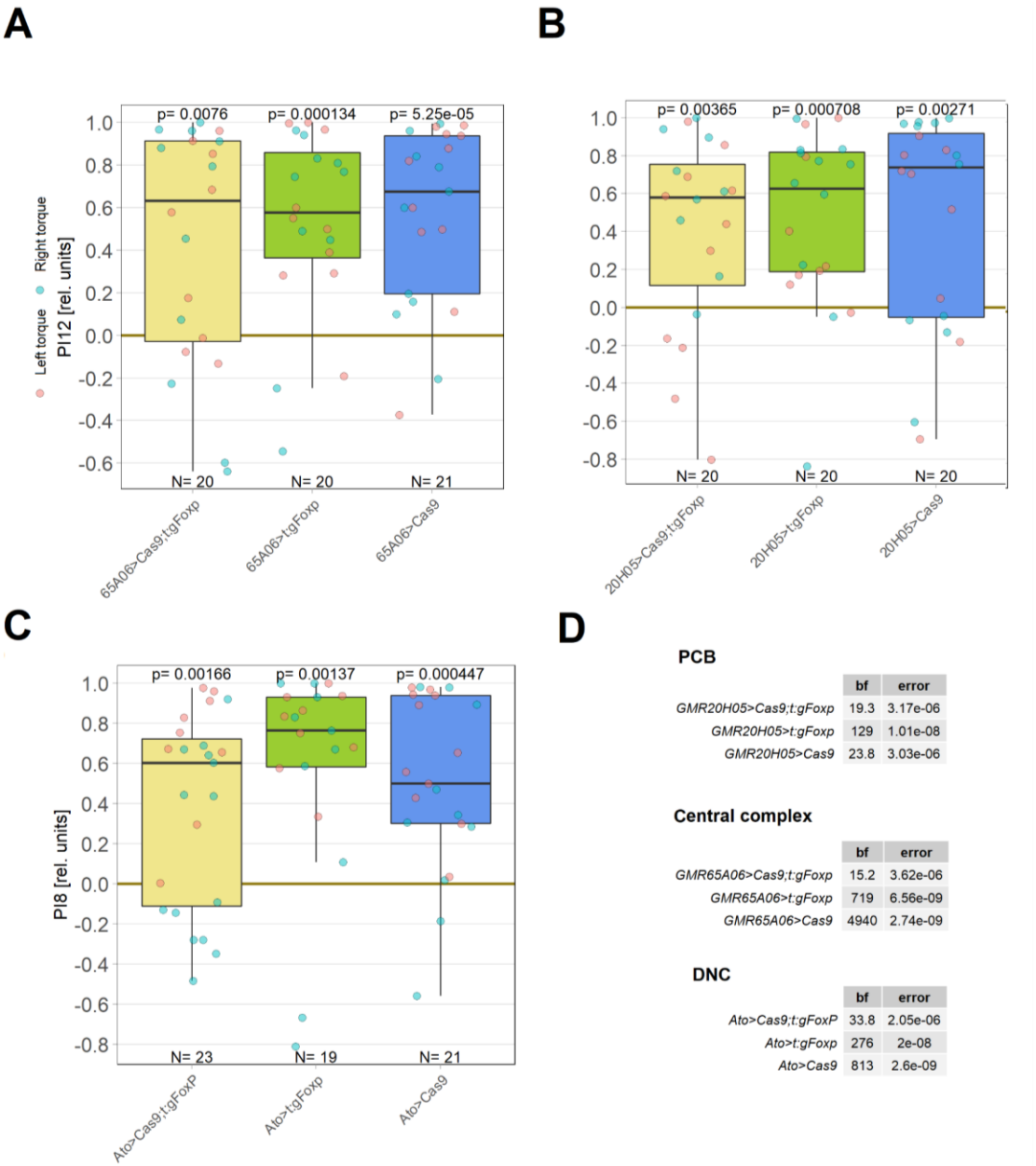

PCB

	bf	error
GMR20H05>Cas9;t:gFoxp	19.3	3.17e-06
GMR20H05>t:gFoxp	129	1.01e-08
GMR20H05>Cas9	23.8	3.03e-06

Central complex

	bf	error
GMR65A06>Cas9;t:gFoxp	15.2	3.62e-06
GMR65A06>t:gFoxp	719	6.56e-09
GMR65A06>Cas9	4940	2.74e-09

DNC

	bf	error
Ato>Cas9;t:gFoxP	33.8	2.05e-06
Ato>t:gFoxp	276	2e-08
Ato>Cas9	813	2.6e-09

Figure 5: For operant self-learning, *FoxP* is likely not required in the brain.

Plotted are performance indices for the first period after training (PI8/12). Each colored dot represents a single fly experiment. Red dots denote experiments where the fly was punished on its left turning torque domain, blue dots denote flies that were punished on their right turning domain. Box plots denote medians, quartiles and non-outlier range. Statistical analyses test for differences of PIs against zero (above plots and D).

Flies with *FoxP* knocked out in the protocerebral bridge (left. yellow) as well as the gRNA (middle, green) and Cas9 (right, blue) control flies show high PIs, large Bayes factors (D) and small p-values, indicating their self-learning is intact. Data: 10.5283/epub.52956

Flies with *FoxP* knocked out in the protocerebral bridge and additional components of the central complex (left. yellow) as well as the gRNA (middle, green) and Cas9 (right, blue) control flies show high PIs, large Bayes factors (D) and small p-values, indicating their self-learning is intact. Data: http://doi.org/10.5283/epub.52951

Flies with *FoxP* knocked out in the dorsal cluster neurons (left. yellow) as well as the gRNA (middle, green) and Cas9 (right, blue) control flies show high PIs, large Bayes factors (D) and small p-values, indicating their self-learning is intact. Data: 10.5283/epub.52946

Bayesian statistics for the three datasets.

We discovered that aPKC is required in MNs for operant self-learning (see above). As *FoxP* is also expressed in MNs, we knocked *FoxP* out in MNs using two different driver lines, C380 and D42. However, CRISPR/Cas9-mediated *FoxP* knock-out in MNs disrupted flight-performance of manipulated flies to an extent that precluded any torque learning experiments. Our results above (Fig. 3) will now allow us to select more specific driver lines, expressing only in the identified wing steering MNs (Ehrhardt et al., 2023), which may yield *FoxP* knock-out flies (or any other manipulation) with sufficient flight performance.

3.5. Temporal genome editing: Self-learning impaired only after a 2-week *FoxP* knockout

FoxP was shown to be important for normal development (Castells-Nobau et al., 2019; Palazzo et al., 2020). Strong motor impairments were reported after a developmental *FoxP* knock-out, for instance rendering the animals unable to fly (see above). Since the ability to fly is a basic requirement for torque learning, we used a CRISPR/Cas9-based approach to pan-neuronally knock out *FoxP* in adult flies. No effect was observed on self-learning two days after the start of the knock-out induction (Fig. 6 A), but waiting for 14 days after the pan-neural knock-out yielded a significant self-learning impairment (Fig. 6B). As a test seven days after induction was also without effect (DOI: 10.5283/epub.52965), self-learning remains functional for at least 7-14 days after cessation of *FoxP* gene transcription in all neurons.

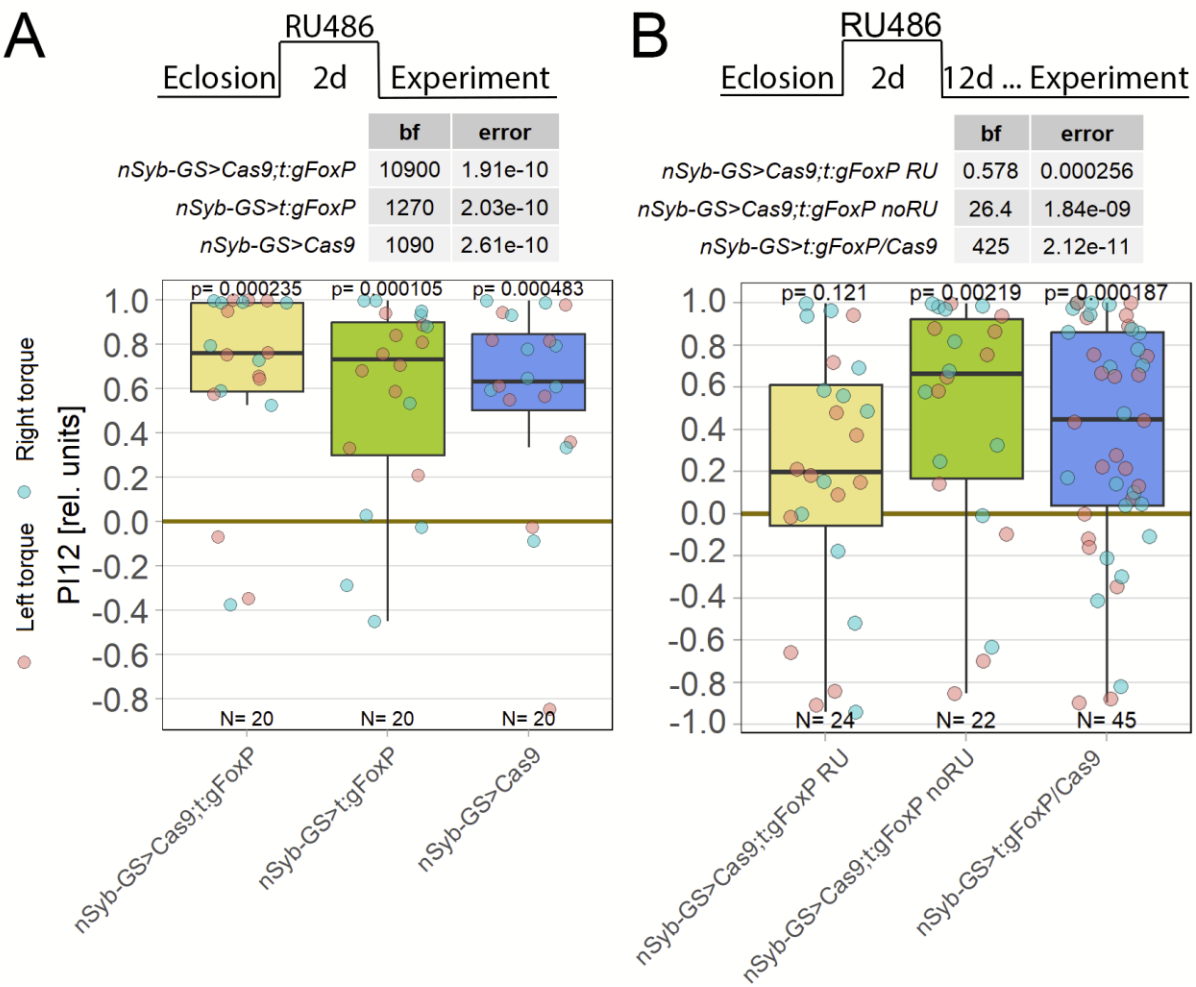

Figure 6: Knockout of *FoxP* in adult *Drosophila* shows learning impairments only after 14 days. Plotted are performance indices for the first period after training (PI12). Each colored dot represents a single fly experiment. Red dots denote experiments where the fly was punished on its left turning torque domain, blue dots denote flies that were punished on their right turning domain. Box plots denote medians, quartiles and non-outlier range. Statistical analyses test for differences of PIs against zero.

A. Self-learning two days after *FoxP* knock-out induction with RU486. Experimental animals (left, yellow) as well as gRNA (middle, green) and Cas9 (left, blue) control animals show all high PIs as well as large Bayes Factors above 1000 and p-values below 0.005, indicating that all groups showed unimpaired self-learning. Data: 10.5283/epub.52963
B. Self-learning 14 days after *FoxP* knock-out induction with RU486 and 12 days after cessation of RU486 administration. Experimental animals (left, yellow) show low PIs as well as a Bayes Factor of less than one together with a large p-value, whereas both the genetic control animals without RU486 treatment (middle, green) and the pooled RU486-treated gRNA and Cas9 controls (right, blue) show high PIs, large Bayes Factors and p-values smaller than 0.005, indicating an impairment in self-learning only in the experimental group. Data: 10.5283/epub.52964

3.6. *αPKC* acts via non-canonical pathways in self-learning

Having established that *αPKC* is required in *FoxP*-positive MNs, we sought to identify fur-

ther components of the *aPKC*-dependent plasticity underlying operant self-learning in *Drosophila*. It is not uncommon for plasticity mechanisms in the adult animal to recruit genes with a function during neuronal development (Greenspan, 1995; Mayford and Kandel, 1999; Leslie and Nedivi, 2011). A prominent interaction partner of *aPKC* during *Drosophila* nervous system development is *bazooka* (*baz*), a crucial component of the highly conserved PAR complex (Pichaud, 2018; Thompson, 2022). However, knocking out *baz* in all adult neurons did not disrupt operant self-learning (Fig. 7A), suggesting that the Par complex signaling pathway is not involved in operant self-learning. A second prominent aPKC interaction partner is the kidney and brain protein (KIBRA) acting in the conserved Hippo pathway (Yoshihama et al., 2011, 2012) and also proposed to be involved in learning/memory (Sacktor, 2012; Heitz et al., 2016; Zlomuzica et al., 2018; Ferguson et al., 2019; Ji et al., 2019). Knocking out KIBRA in all adult neurons also did not disrupt operant self-learning (Fig. 7B).

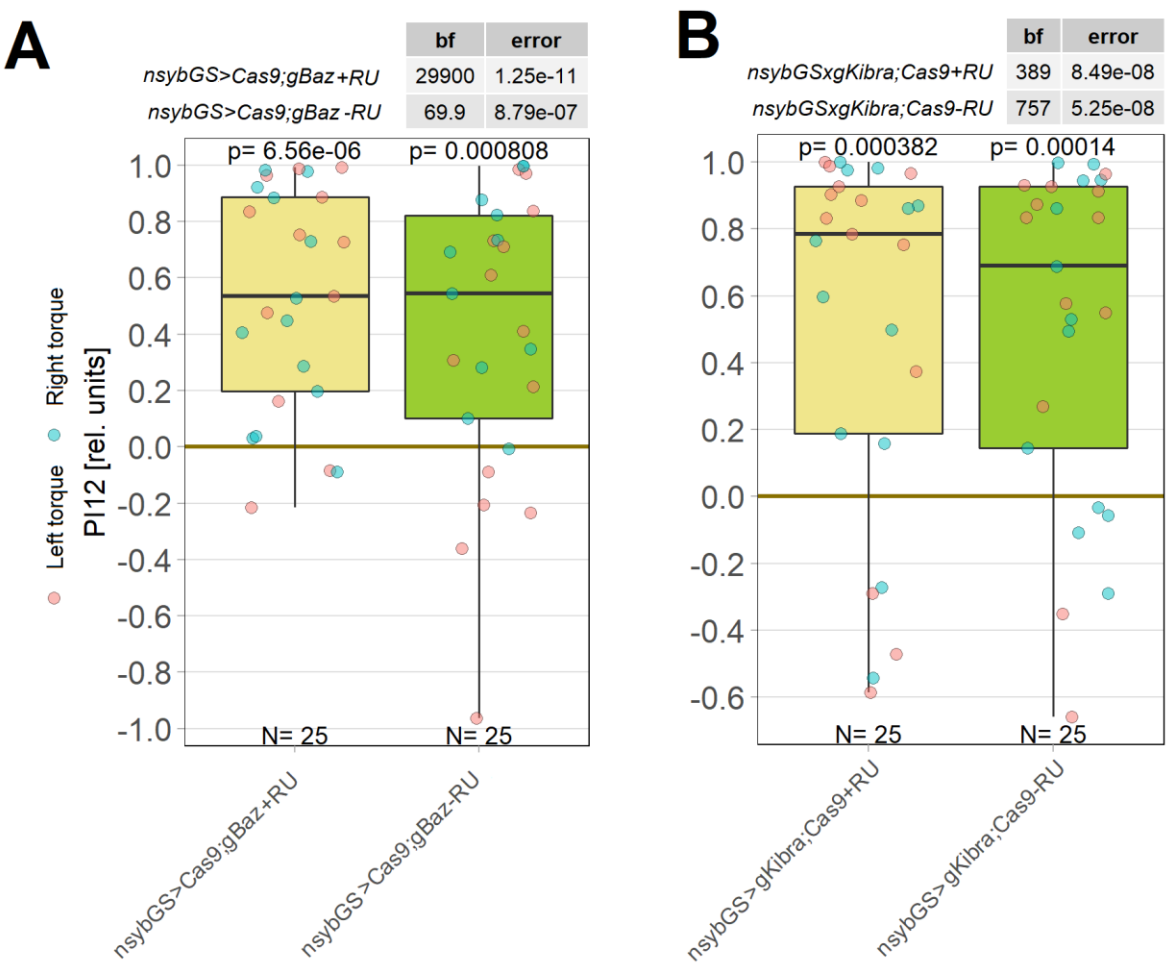

Fig. 7: Neither *bazooka* nor KIBRA are involved in operant self-learning.

Plotted are performance indices for the first period after training (PI12). Each colored dot represents a single fly experiment. Red dots denote experiments where the fly was punished on its left turning torque domain, blue dots denote flies that were punished on their right turning domain. Box plots denote medians, quartiles and non-outlier range. Statistical analyses test for differences of PIs against zero.

A. Knocking out *bazooka* using CRISPR/Cas9-mediated genome editing in adult animals has no effect on operant self-learning. Both flies that were fed the steroid hormone RU486 (left, yellow) and the genetically identical flies without the hormone (right, green), show high PIs, low p-values and high Bayes Factors, indicating a preference for the unpunished torque domain. Data: 10.5283/epub.52947

B. Knocking out KIBRA using CRISPR/Cas9-mediated genome editing in adult animals has no effect on operant self-learning. Both flies that were fed the steroid hormone RU486 (left, yellow) and the genetically identical flies without the hormone (right, green), show high PIs, low p-values and high Bayes Factors, indicating a preference for the unpunished torque domain. Data: 10.5283/epub.53685

4. Discussion

Operant self-learning in *Drosophila* is a form of motor learning that appears to be conserved among bilaterians. The transcription factor *FoxP* is involved in various forms of motor learning in chordates (Lai et al., 2001; Haesler et al., 2007; Groszer et al., 2008; Fisher and Scharff, 2009; Bolhuis et al., 2010; French et al., 2012, 2019; Schreiweis et al., 2014; Day et al., 2019; Co et al., 2020), as is PKC (Sakaguchi and Yamaguchi, 1997; Watanabe et al., 2002, 2006; Metzger and Kapfhammer, 2003; Yoshida et al., 2003; Sakaguchi, 2004; Gallimore et al., 2018). PKC is also involved in motor learning in the feeding behavior of the lophotrochozoan *Aplysia (Lorenzetti et al., 2008)* and both are involved in motor learning in the ecdysozoan *Drosophila* (this work and (Brembs and Plendl, 2008; Mendoza et al., 2014; Colomb and Brembs, 2016). This wealth of evidence supports a 'deep homology' for motor learning in bilaterians (Scharff and Petri, 2011).

In this work, we present new insights into the neurobiological mechanisms underlying this form of motor learning.

4.1. Self-learning requires *aPKC* in *FoxP* wing steering motor neurons

While previous evidence suggested that some PKC activity was required in some MNs for operant self-learning (Colomb and Brembs,

2016), it was not clear which PKC gene was involved and in which MNs. Improving upon the previous attempts to identify the responsible PKC gene, here we used the CRISPR/Cas9 technique to first rule out that *PKC53e* is involved and then show that the atypical PKC (aPKC) is necessary for operant self-learning (Fig. 1). Restricting transgenic manipulations to *FoxP* isoform-B positive neurons and using anatomical experiments to confirm behavioral results suggesting that *FoxP* is not necessary in the brain for operant self-learning (Figs. 2, 5), we now hypothesize that *aPKC* activity is required in aPKC/*FoxP*-positive direct wing steering MNs in the ventral nerve cord (VNC). Our analysis of these direct wing muscles, responsible for, e.g. wing beat amplitude (a major contributing factor to yaw torque) (Dickinson, 2005), revealed *aPKC/FoxP* co-expressing MNs innervating a specific subset of these muscles (Fig. 3), corroborating our hypothesis.

4.2. Motor neurons involved in optomotor responses co-express aPKC and *FoxP*

Specifically, the basalar muscle b1 that is known to regulate wing beat amplitude during optomotor stimulation through phase shifts of its action potential within the wing beat cycle (Heide and Götz, 1996) is innervated by a MN with very strong aPKC and *FoxP* expression in all 11 animals analyzed. Similarly, b3 is also innervated by a MN with very strong aPKC and

FoxP expression and the b3 muscle is reported to increase activity when the ipsilateral wing decreases its amplitude (Lindsay et al., 2017). The b1 and the b3 muscles thus both share similar sizes and morphologies, are innervated by MNs with particularly thick processes and presynaptic active zones, insert at opposite sides of the basalar sclerite and act in a push-pull fashion in controlling wing beat amplitude (Lindsay et al., 2017), a major contributor to yaw torque. Although the MN innervating the third basalar muscle, b2, also expresses aPKC along the axon, we did not detect aPKC signal in axon terminals or active zones, and it does not show *FoxP* label, thus ruling out a function of b2 in aPKC/FoxP mediated operant self-learning. In contrast to b1 and b3, b2 firing is not linked to the wingbeat cycle, but instead, it fires in bursts during turning maneuvers (Whitehead et al., 2022). Corroborating the conclusion that it is not involved in mediating operant self-learning, b2 is silent during straight flight, but it is likely involved in regulating body saccades (Heide, Götz, 1996), which are by themselves not relevant for controlling the heat in our experiments. For the basalar muscles the emerging picture is that b1 and b3 are the top candidates for self-learning because they likely regulate wingbeat amplitude and thus also yaw torque on a wingbeat cycle by cycle basis. Strikingly, the MNs innervating

these two muscles show high levels of aPKC and FoxP expression. Although much less is known about the pterale muscles, and neither iii3 nor iii4 (both with aPKC and FoxP co-expression) have been recorded electrophysiologically during flight, a similar picture starts emerging. The MN to the left muscle i1 is known to be active during right turns (Heide and Götz, 1996) and co-expresses aPKC and FoxP, whereas iii1 does reportedly (Heide and Götz, 1996) not participate in optomotor responses and is innervated by a MN with weak aPKC and no *FoxP* label. In sum, flight steering muscles that are known to regulate flight steering in response to optomotor stimulation receive aPKC and *FoxP* positive motor innervation.

4.3. Operant self-learning modifies optomotor responses

Given that MNs innervating muscles important for controlling wingbeat amplitudes during optomotor responses are co-expressing aPKC and *FoxP*, the genes important for our operant experiments where the animals learn to generate specific wingbeat amplitudes, a straightforward hypothesis emerges: if operant self-learning permanently altered the properties of MNs that are involved in optomotor responses, we should be able to observe training-induced modifications in the flies' optomotor behavior after training. Analyzing

the optomotor responses of a separate cohort of wild type flies corroborated this hypothesis (Fig. 4). The optomotor magnitude was reduced on the punished turning direction, but unaltered on the punished direction. About a third of the variance in the torque preference after training can be explained by this optomotor asymmetry.

Plasticity in steering movements such as optomotor responses have been observed before, such as in classic “inversion goggles” experiments where the coupling between the fly’s movements and the environment was reversed (Wolf and Heisenberg, 1986) or in a more recent experiment revealing adaptation processes (Mano et al., 2023). However, the effect of operant conditioning of spontaneous torque fluctuations on elicited optomotor responses was unexpected. So unexpected, in fact, that our study, triggered by the expression results (Figs. 2, 3), is the first one to analyze optomotor responses after conditioning since the initial description of these operant experiments (Wolf and Heisenberg, 1991), even though that capability existed from the very beginning.

4.4. Motoneuron plasticity mediates operant self-learning

Taken together, these results converge on the hypothesis that plasticity in MNs that innervate the direct muscles involved in generating yaw torque, but not other steering MNs, mediates operant self-learning in *Drosophila*. The importance of MN plasticity is emphasized by *FoxP*-dependent plasticity apparently not being required in the brain (Fig. 5). This MN plasticity could either be implemented by (a) postsynaptic plasticity of the input synapses to these MNs, postsynaptic because the MNs but not the interneurons express the proteins required for self-learning, or (b) on the level of the intrinsic excitability of flight steering motoneurons, or (c) on the level of the output synapses to the respective steering muscles. However, the mechanism and the subcellular localization of self-learning in MNs remains to be determined.

A second interesting, but so far unstudied population of *αPKC/FoxP* co-expressing neurons resides in the abdominal neuromer of the VNC. As flies use their abdomen analogously to a rudder during turns in flight (Götz et al., 1979; Zanker, 1988), involvement of these neurons seems plausible in addition to wing MNs.

While few studies in insects have shown MN plasticity, the *Aplysia* sensorimotor synapse is a classical model for research on plasticity mechanisms. There is a rich literature on MN plasticity in this preparation, some of which reports PKC-dependent mechanisms (Cai et al., 2008; Fulton et al., 2008; Glanzman, 2008; Villareal et al., 2009; Reissner et al., 2010; Jin et al., 2011; Bougie et al., 2012; Choi et al., 2014; Hu et al., 2015, 2017a; Ferguson et al., 2019; Alexandrescu and Carew, 2020). Also in mammals (including humans) MN plasticity in the spinal cord is a readily observable phenomenon in non-clinical and clinical settings (Wolpaw and Lee, 1989; Wolpaw et al., 1989; Carp and Wolpaw, 1994; Carp et al., 2001; Wang et al., 2006; Wolpaw, 2012; Eftekhar et al., 2018; Kaneko et al., 2022; Rochat et al., 2022; Simonyan et al., 2022). The discovery of aPKC-dependent plasticity in *Drosophila* MNs expands this body of literature to a genetically tractable organism and inasmuch as clinical practice relies on MN plasticity, may even help instruct the development of clinical applications.

Until our work, in flies, PKC activity has only been shown to be important for memory consolidation/maintenance in world-learning experiments, but not for learning/acquisition (Kane et al., 1997; Drier et al., 2002). Also in *Dro-*

sophila at the torque meter, PKCs are dispensable for world-learning (Brembs and Plendl, 2008). Similarly, in different forms of world-learning in *Aplysia*, aPKC is thought to be involved in memory consolidation or maintenance, but leaving learning intact (Michel et al., 2011; Bougie et al., 2012; Hu et al., 2017a, 2017b; Lyons et al., 2017; Sacktor and Hell, 2017). Also in vertebrates, most reports cite the role of PKC in memory, rather than learning (Sacktor, 2012; Sacktor and Hell, 2017; Gao et al., 2018). While in some of these processes the type of PKC is not known, in others atypical PKCs are involved, and in yet others classical PKCs. In the literature, there does not appear to be a clear picture of a single form of PKC-mediated plasticity, even though several strands of similarity can be discerned between processes. Notably, the one other preparation where PKC activity has been linked to learning rather than memory, is also conceptually most closely resembling the one we used here, operant reward learning in *Aplysia* feeding behavior. However, in this preparation, the calcium-dependent Apl-I PKC not the atypical Apl-III PKC appears to be mediating the plasticity (Lorenzetti et al., 2008). Given the degeneracy between the different PKC genes and the fact that they not only can compensate for long-term PKCi-mediated inhibition (this work and (Colomb and Brembs, 2016), but also for each

other (Tsokas et al., 2016), more research is needed to elucidate how these different mechanisms of plasticity evolved and are related to each other.

It has long been recognized that insects with asymmetrical wing damage need to adjust the neural commands for generating torque to compensate for the changed physical torque (e.g., (Heisenberg and Wolf, 1993; Haas and Cartar, 2008; Fernández et al., 2012; Vance and Roberts, 2014; Kassner et al., 2016)). Plasticity in wing steering motor neurons provides a potential mechanism for such adjustments.

4.5. Self-learning is mediated by a non-canonical *aPKC/FoxP* pathway

Neither *bazooka* (*baz*) nor the kidney and brain gene (KIBRA), two prominent interaction partners of aPKC (Wieschaus and Noell, 1986; Yoshihama et al., 2011, 2012; Sacktor, 2012; Heitz et al., 2016; Soriano et al., 2016; Pichaud, 2018; Zlomuzica et al., 2018; Ferguson et al., 2019; Thompson, 2022), showed an effect on operant self-learning when they were knocked out in the adult (Fig. 7), potentially raising doubts about the effectiveness of the CRISPR/Cas9 method in these cases. However, we have ensured that both manipulations successfully knocked out the genes. First, we found that the *baz* knock-out, rather than im-

pairing self-learning, increases learning performance (manuscript in preparation), suggesting the PAR complex may be sequestering *aPKC* and thereby limiting its availability for self-learning. Our KIBRA knock-out had a severe effect on flight performance when elicited during development, suggesting that also this manipulation was, in principle, effective. Interestingly, at least during development, *baz* and KIBRA have been reported to have opposite effects on the function of *aPKC*, with the PAR complex (*baz*) and the Hippo pathway (KIBRA) mutually inhibiting each other (Zhang and Wei, 2022). While *baz* is thought to mediate *aPKC* activity, KIBRA is thought to exert negative regulatory activity on *aPKC*. Thus, knocking out each one of them should have revealed a decrement in self-learning in at least one of them, if the processes during development were recapitulated during self-learning. On the other hand, experiments in which KIBRA has been shown to be involved in learning/memory, have suggested a positive rather than a negative regulatory role (Hu et al., 2017b; Ferguson et al., 2019), albeit with an emphasis on long-term memory rather than learning (Zha and Sossin, 2022). Whichever way *aPKC* may be interacting with components of these canonical pathways, the literature predicts that at least one of our manipulations should have revealed a decrement in operant self-learning. The fact that this

prediction was falsified strongly suggests that *aPKC* exerts its function in a non-canonical manner in operant self-learning plasticity. We are currently pursuing research on the possibility that *bazooka* may constitute a negative regulator of aPKC activity in operant self-learning.

4.6. Persistent *FoxP* effect on operant self-learning in adults

As *FoxP* mutants are impaired in operant self-learning (Mendoza et al., 2014), two hypotheses about the role of the prominent transcription factor arise. First, *FoxP* may be directly involved in the learning process via some unknown, cytosolic function. A transcription factor function appears unlikely, due to the short duration of our experiments. Second, *FoxP* may exert its effects as a developmental regulator, being crucial for the development of the circuits mediating operant self-learning. As the developmental role of FoxP genes is well documented (Takahashi et al., 2009; Bowers et al., 2014; Rocca et al., 2017; Castells-Nobau et al., 2019; Co et al., 2020; Palazzo et al., 2020) and there are few domains in the gene that would lend themselves for a hypothetical cytosolic function, the latter hypothesis appeared more plausible. The result that adult knockout of *FoxP* had no immediate effect in operant self-learning (Fig. 6A) seemed to corroborate this

hypothesis. In contrast, supporting a continued role of FoxP genes in motor learning also after development are data from songbirds where *FoxP2* gene expression is not only regulated by singing (Teramitsu and White, 2006; Teramitsu et al., 2010; Chen et al., 2013; Thompson et al., 2013), but where normal *FoxP2* expression is necessary in adults to maintain learned song (Day et al., 2019; Xiao et al., 2021). To also test the second hypothesis, we aged the flies after the *FoxP* knockout and tested them 7 and 14-days later. Flies still showed operant self-learning after seven days without *FoxP* transcription (DOI: 10.5283/epub.52965), but were impaired after 14 days (Fig. 6B). These results suggest a role of adult *FoxP* expression in maintaining operant self-learning capabilities after development, analogous to the role of FoxP2 in songbird vocal learning (Day et al., 2019; Xiao et al., 2021). This result may be explained by the temporal dynamics of the genes regulated by *FoxP (Kuo et al., 2023)*.

Acknowledgements: We thank Thomas Kopp in the electronics workshop of the University of Regensburg, without whose tireless support this work could not have been accomplished. We are indebted to Michael Krahn for very helpful feedback on PKC interaction partners and for sending us his KIBRA gRNA flies before publication. We thank the DFG for financial support: DFG BR 1892/17-1. This work is dedicated to the late Jochen Pflüger, at whose memorial CD and BB agreed to collaborate on motor neurons.

5. References

Alexandrescu A, Carew TJ (2020) Postsynaptic effects of cysteine-rich neurotrophic factor in the induction of activity-dependent long-term facilitation in. Learn Mem 27:124–129.

Arendt D (2021) Elementary nervous systems. Philos Trans R Soc Lond B Biol Sci 376:20200347.

Azevedo A et al. (2022) Tools for comprehensive reconstruction and analysis of*Drosophila*motor circuits. bioRxiv Available at: http://biorxiv.org/lookup/doi/10.1101/2022.12.15.520299.

Benjamin DJ et al. (2018) Redefine statistical significance. Nat Hum Behav 2:6–10.

Bolhuis JJ, Okanoya K, Scharff C (2010) Twitter evolution: converging mechanisms in birdsong and human speech. Nat Rev Neurosci 11:747–759.

Bougie JK, Cai D, Hastings M, Farah CA, Chen S, Fan X, McCamphill PK, Glanzman DL, Sossin WS (2012) Serotonin-induced cleavage of the atypical protein kinase C Apl III in Aplysia. J Neurosci 32:14630–14640.

Bowers JM, Perez-Pouchoulen M, Roby CR, Ryan TE, McCarthy MM (2014) Androgen modulation of Foxp1 and Foxp2 in the developing rat brain: impact on sex specific vocalization. Endocrinology 155:4881–4894.

Brembs B (2008) Operant learning of Drosophila at the torque meter. J Vis Exp Available at: http://dx.doi.org/10.3791/731.

Brembs B (2009) Mushroom bodies regulate habit formation in Drosophila. Curr Biol 19:1351–1355.

Brembs B (2011) Spontaneous decisions and operant conditioning in fruit flies. Behav Processes 87:157–164.

Brembs B, Hempel de Ibarra N (2006) Different parameters support generalization and discrimination learning in Drosophila at the flight simulator. Learn Mem 13:629–637.

Brembs B, Plendl W (2008) Double dissociation of PKC and AC manipulations on operant and classical learning in Drosophila. Curr Biol 18:1168–1171.

Brembs B, Wiener J (2006) Context and occasion setting in Drosophila visual learning. Learn Mem 13:618–628.

Cai D, Chen S, Glanzman DL (2008) Postsynaptic regulation of long-term facilitation in Aplysia. Curr Biol 18:920–925.

Carp JS, Chen XY, Sheikh H, Wolpaw JR (2001) Operant conditioning of rat H-reflex affects motoneuron axonal conduction velocity. Exp Brain Res 136:269–273.

Carp JS, Wolpaw JR (1994) Motoneuron plasticity underlying operantly conditioned decrease in primate H-reflex. J Neurophysiol 72:431–442.

Castells-Nobau A, Eidhof I, Fenckova M, Brenman-Suttner DB, Scheffer-de Gooyert JM, Christine S, Schellevis RL, van der Laan K, Quentin C, van Ninhuijs L, Hofmann F, Ejsmont R, Fisher SE, Kramer JM, Sigrist SJ, Simon AF, Schenck A (2019) Conserved regulation of neurodevelopmental processes and behavior by FoxP in Drosophila. PLoS One 14:e0211652.

Chen Q, Heston JB, Burkett ZD, White SA (2013) Expression analysis of the speech-related genes FoxP1 and FoxP2 and their relation to singing behavior in two songbird species. J Exp Biol 216:3682–3692.

Choi Y-B, Kadakkuzha BM, Liu X-A, Akhmedov K, Kandel ER, Puthanveettil SV (2014) Huntingtin is critical both pre- and postsynaptically for long-term learning-related synaptic plasticity in Aplysia. PLoS One 9:e103004.

Colomb J, Brembs B (2010) The biology of psychology: “Simple” conditioning? Commun Integr Biol 3:142–145.

Colomb J, Brembs B (2016) PKC in motorneurons underlies self-learning, a form of motor learning in Drosophila. PeerJ 4:e1971.

Co M, Anderson AG, Konopka G (2020) FOXP transcription factors in vertebrate brain development, function, and disorders. Wiley Interdiscip Rev Dev Biol 9:e375.

Day NF, Hobbs TG, Heston JB, White SA (2019) Beyond Critical Period Learning: Striatal FoxP2 Affects the Active Maintenance of Learned Vocalizations in Adulthood. eNeuro 6 Available at: http://dx.doi.org/10.1523/ENEURO.0071-19.2019.

Dickinson MH (2005) The initiation and control of rapid flight maneuvers in fruit flies. Integr Comp Biol 45:274–281.

Dickinson MH, Tu MS (1997) The function of dipteran flight muscle. Comp Biochem Physiol A Comp Physiol 116:223–238.

Drier EA, Tello MK, Cowan M, Wu P, Blace N, Sacktor TC, Yin JCP (2002) Memory enhancement and formation by atypical PKM activity in Drosophila melanogaster. Nat Neurosci 5:316–324.

Du Y, Krakauer JW, Haith AM (2022) The relationship between habits and motor skills in humans. Trends Cogn Sci 26:371–387.

Eftekhar A, Norton JJS, McDonough CM, Wolpaw JR (2018) Retraining Reflexes: Clinical Translation of Spinal Reflex Operant Conditioning. Neurotherapeutics 15:669–683.

1445 Ehrhardt E, Whitehead SC, Namiki S, Minegishi R, Siwanowicz I, Feng K, Otsuna H, Fly-
1446 Light Project Team, Meissner GW, Stern D, Truman J, Shepherd D, Dickinson MH, Ito
1447 K, Dickson BJ, Cohen I, Card GM, Korff W (2023) Single-cell type analysis of wing pre-
1448 motor circuits in the ventral nerve cord of. bioRxiv Available at:
1449 http://dx.doi.org/10.1101/2023.05.31.542897.

1450 Ferguson L, Hu J, Cai D, Chen S, Dunn TW, Pearce K, Glanzman DL, Schacher S, Sossin WS
1451 (2019) Isoform Specificity of PKMs during Long-Term Facilitation in Is Mediated
1452 through Stabilization by KIBRA. J Neurosci 39:8632–8644.

1453 Fernández MJ, Springthorpe D, Hedrick TL (2012) Neuromuscular and biomechanical
1454 compensation for wing asymmetry in insect hovering flight. J Exp Biol 215:3631–
1455 3638.

1456 Fisher SE, Scharff C (2009) FOXP2 as a molecular window into speech and language.
1457 Trends Genet 25:166–177.

1458 French CA, Jin X, Campbell TG, Gerfen E, Groszer M, Fisher SE, Costa RM (2012) An aetio-
1459 logical Foxp2 mutation causes aberrant striatal activity and alters plasticity during
1460 skill learning. Mol Psychiatry 17:1077–1085.

1461 French CA, Vinueza Veloz MF, Zhou K, Peter S, Fisher SE, Costa RM, De Zeeuw CI (2019)
1462 Differential effects of Foxp2 disruption in distinct motor circuits. Mol Psychiatry
1463 24:447–462.

1464 Fresco N, Tzelgov J, Shmuelof L (2022) How can caching explain automaticity? Psychon
1465 Bull Rev Available at: http://dx.doi.org/10.3758/s13423-022-02191-0.

1466 Fulton D, Condro MC, Pearce K, Glanzman DL (2008) The potential role of postsynaptic
1467 phospholipase C activity in synaptic facilitation and behavioral sensitization in Ap-
1468 lysia. J Neurophysiol 100:108–116.

1469 Gallimore AR, Kim T, Tanaka-Yamamoto K, De Schutter E (2018) Switching On Depres-
1470 sion and Potentiation in the Cerebellum. Cell Rep 22:722–733.

1471 Gao PP, Goodman JH, Sacktor TC, Francis JT (2018) Persistent Increases of PKMζ in Sen-
1472 sorimotor Cortex Maintain Procedural Long-Term Memory Storage. iScience 5:90–
1473 98.

1474 Glanzman DL (2008) New tricks for an old slug: the critical role of postsynaptic mecha-
1475 nisms in learning and memory in Aplysia. Prog Brain Res 169:277–292.

1476 Götz KG (1964) [Optomoter studies of the visual system of several eye mutants of the
1477 fruit fly Drosophila]. Kybernetik 2:77–92.

1478 Götz KG, Hengstenberg B, Biesinger R (1979) Optomotor control of wing beat and body
1479 posture in drosophila. Biol Cybern 35:101–112.

1480 Greenspan RJ (1995) Flies, genes, learning, and memory. Neuron 15:747–750.

1481 Groszer M et al. (2008) Impaired synaptic plasticity and motor learning in mice with a
1482 point mutation implicated in human speech deficits. Curr Biol 18:354–362.

1483 Guo A, Li L, Xia SZ, Feng CH, Wolf R, Heisenberg M (1996) Conditioned visual flight orien-
1484 tation in Drosophila: dependence on age, practice, and diet. Learn Mem 3:49–59.

1485 Haas CA, Cartar RV (2008) Robust flight performance of bumble bees with artificially in-
1486 duced wing wear. Can J Zool 86:668–675.

1487 Haesler S, Rochefort C, Georgi B, Licznerski P, Osten P, Scharff C (2007) Incomplete and
1488 inaccurate vocal imitation after knockdown of FoxP2 in songbird basal ganglia nu-
1489 cleus Area X. PLoS Biol 5:e321.

1490 Heide G, Götz KG (1996) Optomotor control of course and altitude in Drosophila mela-
1491 nogaster is correlated with distinct activities of at least three pairs of flight steering
1492 muscles. J Exp Biol 199:1711–1726.

1493 Heisenberg M, Wolf R (1993) The sensory-motor link in motion-dependent flight control
1494 of flies. Rev Oculomot Res 5:265–283.

1495 Heitz FD, Farinelli M, Mohanna S, Kahn M, Duning K, Frey MC, Pavenstädt H, Mansuy IM
1496 (2016) The memory gene KIBRA is a bidirectional regulator of synaptic and struc-
1497 tural plasticity in the adult brain. Neurobiol Learn Mem 135:100–114.

1498 Hiroki S, Iino Y (2022) The redundancy and diversity between two novel PKC isotypes
1499 that regulate learning in. Proc Natl Acad Sci U S A 119 Available at:
1500 http://dx.doi.org/10.1073/pnas.2106974119.

1501 Hu J, Adler K, Farah CA, Hastings MH, Sossin WS, Schacher S (2017a) Cell-Specific PKM
1502 Isoforms Contribute to the Maintenance of Different Forms of Persistent Long-Term
1503 Synaptic Plasticity. J Neurosci 37:2746–2763.

1504 Hu J, Ferguson L, Adler K, Farah CA, Hastings MH, Sossin WS, Schacher S (2017b) Selec-
1505 tive Erasure of Distinct Forms of Long-Term Synaptic Plasticity Underlying Different
1506 Forms of Memory in the Same Postsynaptic Neuron. Curr Biol 27:1888–1899.e4.

1507 Hu J-Y, Levine A, Sung Y-J, Schacher S (2015) cJun and CREB2 in the postsynaptic neuron
1508 contribute to persistent long-term facilitation at a behaviorally relevant synapse. J
1509 Neurosci 35:386–395.

1510 Jékely G (2021) The chemical brain hypothesis for the origin of nervous systems. Philos
1511 Trans R Soc Lond B Biol Sci 376:20190761.

1512 Jin I, Kandel ER, Hawkins RD (2011) Whereas short-term facilitation is presynaptic, inter-
1513 mediate-term facilitation involves both presynaptic and postsynaptic protein ki-
1514 nases and protein synthesis. Learn Mem 18:96–102.

1515 Ji Z, Li H, Yang Z, Huang X, Ke X, Ma S, Lin Z, Lu Y, Zhang M (2019) Kibra Modulates Learn-
1516 ing and Memory via Binding to Dendrin. Cell Rep 26:2064–2077.e7.

1517 Kaneko N, Sasaki A, Yokoyama H, Masugi Y, Nakazawa K (2022) Effects of action obser-
1518 vation and motor imagery of walking on the corticospinal and spinal motoneuron
1519 excitability and motor imagery ability in healthy participants. PLoS One
1520 17:e0266000.

1521 Kane NS, Robichon A, Dickinson JA, Greenspan RJ (1997) Learning without performance
1522 in PKC-deficient Drosophila. Neuron 18:307–314.

1523 Kassner Z, Dafni E, Ribak G (2016) Kinematic compensation for wing loss in flying dam-
1524 selflies. J Insect Physiol 85:1–9.

1525 Keijzer F, van Duijn M, Lyon P (2013) What nervous systems do: early evolution, input–
1526 output, and the skin brain thesis. Adapt Behav 21:67–85.

1527 Kittel RJ, Wichmann C, Rasse TM, Fouquet W, Schmidt M, Schmid A, Wagh DA, Pawlu C,
1528 Kellner RR, Willig KI, Hell SW, Buchner E, Heckmann M, Sigrist SJ (2006) Bruchpilot
1529 promotes active zone assembly, Ca2+ channel clustering, and vesicle release. Sci-
1530 ence 312:1051–1054.

1531 Krakauer JW, Hadjiosif AM, Xu J, Wong AL, Haith AM (2019) Motor Learning. Compr Phys-
1532 iol 9:613–663.

1533 Kuo H-Y, Chen S-Y, Huang R-C, Takahashi H, Lee Y-H, Pang H-Y, Wu C-H, Graybiel AM, Liu
1534 F-C (2023) Speech- and language-linked FOXP2 mutation targets protein motors in
1535 striatal neurons. Brain Available at: http://dx.doi.org/10.1093/brain/awad090.

1536 Lai CS, Fisher SE, Hurst JA, Vargha-Khadem F, Monaco AP (2001) A forkhead-domain
1537 gene is mutated in a severe speech and language disorder. Nature 413:519–523.

1538 Leslie JH, Nedivi E (2011) Activity-regulated genes as mediators of neural circuit plastic-
1539 ity. Prog Neurobiol 94:223–237.

1540 Lindsay T, Sustar A, Dickinson M (2017) The Function and Organization of the Motor Sys-
1541 tem Controlling Flight Maneuvers in Flies. Curr Biol 27:345–358.

1542 Liu G, Seiler H, Wen A, Zars T, Ito K, Wolf R, Heisenberg M, Liu L (2006) Distinct memory
1543 traces for two visual features in the Drosophila brain. Nature 439:551–556.

1544 Liu L, Wolf R, Ernst R, Heisenberg M (1999) Context generalization in Drosophila visual
1545 learning requires the mushroom bodies. Nature 400:753–756.

1546 Lorenzetti FD, Baxter DA, Byrne JH (2008) Molecular mechanisms underlying a cellular
1547 analog of operant reward learning. Neuron 59:815–828.

1548 Lozano R, Gbekie C, Siper PM, Srivastava S, Saland JM, Sethuram S, Tang L, Drapeau E,
1549 Frank Y, Buxbaum JD, Kolevzon A (2021) FOXP1 syndrome: a review of the literature
1550 and practice parameters for medical assessment and monitoring. J Neurodev Dis-
1551 ord 13:18.

1552 Lyons LC, Gardner JS, Lentsch CT, Gandour CE, Krishnan HC, Noakes EJ (2017) Differen-
1553 tial role of calpain-dependent protein cleavage in intermediate and long-term oper-
1554 ant memory in Aplysia. Neurobiol Learn Mem 137:134–141.

1555 Mano O, Choi M, Tanaka R, Creamer MS, Matos NCB, Shomar JW, Badwan BA, Clandinin
1556 TR, Clark DA (2023) Long-timescale anti-directional rotation in optomotor behavior.
1557 Elife 12 Available at: http://dx.doi.org/10.7554/eLife.86076.

1558 Mayford M, Kandel ER (1999) Genetic approaches to memory storage. Trends Genet
1559 15:463–470.

1560 Mendoza E, Colomb J, Rybak J, Pflüger H-J, Zars T, Scharff C, Brembs B (2014) Drosophila
1561 FoxP mutants are deficient in operant self-learning. PLoS One 9:e100648.

1562 Metzger F, Kapfhammer JP (2003) Protein kinase C: its role in activity-dependent
1563 Purkinje cell dendritic development and plasticity. Cerebellum 2:206–214.

1564 Michel M, Green CL, Lyons LC (2011) PKA and PKC are required for long-term but not
1565 short-term in vivo operant memory in Aplysia. Learn Mem 18:19–23.

1566 Palazzo O, Rass M, Brembs B (2020) Identification of circuits involved in locomotion and
1567 object fixation in. Open Biol 10:200295.

1568 Phelps JS, Hildebrand DGC, Graham BJ, Kuan AT, Thomas LA, Nguyen TM, Buhmann J,
1569 Azevedo AW, Sustar A, Agrawal S, Liu M, Shanny BL, Funke J, Tuthill JC, Lee W-CA
1570 (2021) Reconstruction of motor control circuits in adult Drosophila using automated
1571 transmission electron microscopy. Cell 184:759–774.e18.

1572 Pichaud F (2018) PAR-Complex and Crumbs Function During Photoreceptor Morphogen-
1573 esis and Retinal Degeneration. Front Cell Neurosci 12:90.

1574 Reissner KJ, Pu L, Schaffhausen JH, Boyle HD, Smith IF, Parker I, Carew TJ (2010) A novel
1575 postsynaptic mechanism for heterosynaptic sharing of short-term plasticity. J Neu-
1576 rosci 30:8797–8806.

1577 Rocca DL, Wilkinson KA, Henley JM (2017) SUMOylation of FOXP1 regulates transcrip-
1578 tional repression via CtBP1 to drive dendritic morphogenesis. Sci Rep 7:877.

1579 Rochat C, Bernard-Marissal N, Källstig E, Pradervand S, Perrin FE, Aebischer P, Raoul C,
1580 Schneider BL (2022) Astrocyte-targeting RNA interference against mutated superox-
1581 ide dismutase 1 induces motoneuron plasticity and protects fast-fatigable motor
1582 units in a mouse model of amyotrophic lateral sclerosis. Glia 70:842–857.

1583 Rochefort C, Arabo A, André M, Poucet B, Save E, Rondi-Reig L (2011) Cerebellum shapes
1584 hippocampal spatial code. Science 334:385–389.

1585 Sacktor TC (2012) Memory maintenance by PKMζ--an evolutionary perspective. Mol
1586 Brain 5:31.

1587 Sacktor TC, Hell JW (2017) The genetics of PKMζ and memory maintenance. Sci Signal 10

1588 Available at: http://dx.doi.org/10.1126/scisignal.aao2327.

1589 Sakaguchi H (2004) Effect of social factors on the development of PKC expression in
1590 songbird brain. Neuroreport 15:2819–2823.

1591 Sakaguchi H, Yamaguchi A (1997) Early song-deprivation affects the expression of pro-
1592 tein kinase C in the song control nuclei of the zebra finch during a sensitive period
1593 of song learning. Neuroreport 8:2645–2650.

1594 Salmon DP, Butters N (1995) Neurobiology of skill and habit learning. Curr Opin Neuro-
1595 biol 5:184–190.

1596 Scharff C, Petri J (2011) Evo-devo, deep homology and FoxP2: implications for the evolu-
1597 tion of speech and language. Philos Trans R Soc Lond B Biol Sci 366:2124–2140.

1598 Schreiweis C, Bornschein U, Burguière E, Kerimoglu C, Schreiter S, Dannemann M, Goyal
1599 S, Rea E, French CA, Puliyadi R, Groszer M, Fisher SE, Mundry R, Winter C, Hevers W,
1600 Pääbo S, Enard W, Graybiel AM (2014) Humanized Foxp2 accelerates learning by en-
1601 hancing transitions from declarative to procedural performance. Proc Natl Acad Sci
1602 U S A 111:14253–14258.

1603 Simonyan K, Avetisyan L, Isoyan A, Chavushyan V (2022) Plasticity in Motoneurons Fol-
1604 lowing Spinal Cord Injury in Fructose-induced Diabetic Rats. J Mol Neurosci 72:888–
1605 899.

1606 Soriano EV, Ivanova ME, Fletcher G, Riou P, Knowles PP, Barnouin K, Purkiss A,
1607 Kostelecky B, Saiu P, Linch M, Elbediwy A, Kjær S, O'Reilly N, Snijders AP, Parker PJ,
1608 Thompson BJ, McDonald NQ (2016) aPKC Inhibition by Par3 CR3 Flanking Regions
1609 Controls Substrate Access and Underpins Apical-Junctional Polarization. Dev Cell
1610 38:384–398.

1611 Takahashi H, Takahashi K, Liu F-C (2009) FOXP genes, neural development, speech and
1612 language disorders. Adv Exp Med Biol 665:117–129.

1613 Tang S, Juusola M (2010) Intrinsic activity in the fly brain gates visual information during
1614 behavioral choices. PLoS One 5:e14455.

1615 Teegala LR, Elshoweikh Y, Gudneppanavar R, Thodeti S, Pokhrel S, Southard E, Thodeti
1616 CK, Paruchuri S (2022) Protein Kinase C α and β compensate for each other to pro-
1617 mote stem cell factor-mediated KIT phosphorylation, mast cell viability and prolifer-
1618 ation. FASEB J 36:e22273.

1619 Teramitsu I, Poopatanapong A, Torrisi S, White SA (2010) Striatal FoxP2 is actively regu-
1620 lated during songbird sensorimotor learning. PLoS One 5:e8548.

1621 Teramitsu I, White SA (2006) FoxP2 regulation during undirected singing in adult song-
1622 birds. J Neurosci 26:7390–7394.

1623 Thompson BJ (2022) Par-3 family proteins in cell polarity & adhesion. FEBS J 289:596–
1624 613.

1625 Thompson CK, Schwabe F, Schoof A, Mendoza E, Gampe J, Rochefort C, Scharff C (2013)
1626 Young and intense: FoxP2 immunoreactivity in Area X varies with age, song stereo-
1627 typy, and singing in male zebra finches. Front Neural Circuits 7:24.

1628 Trimarchi JR, Schneiderman AM (1994) The motor neurons innervating the direct flight
1629 muscles of Drosophila melanogaster are morphologically specialized. J Comp Neu-
1630 rol 340:427–443.

1631 Trzesniewski J, Altmann S, Jäger L, Kapfhammer JP (2019) Reduced Purkinje cell size is
1632 compatible with near normal morphology and function of the cerebellar cortex in a
1633 mouse model of spinocerebellar ataxia. Exp Neurol 311:205–212.

1634 Tsokas P, Hsieh C, Yao Y, Lesburguères E, Wallace EJC, Tcherepanov A, Jothianandan D,
1635 Hartley BR, Pan L, Rivard B, Farese RV, Sajan MP, Bergold PJ, Hernández AI, Cottrell
1636 JE, Shouval HZ, Fenton AA, Sacktor TC (2016) Compensation for PKMζ in long-term
1637 potentiation and spatial long-term memory in mutant mice. Elife 5 Available at:
1638 http://dx.doi.org/10.7554/eLife.14846.

1639 Tu MS, Dickinson MH (1996) The control of wing kinematics by two steering muscles of
1640 the blowfly (Calliphora vicina). J Comp Physiol A 178:813–830.

1641 Vance JT, Roberts SP (2014) The effects of artificial wing wear on the flight capacity of the
1642 honey bee Apis mellifera. J Insect Physiol 65:27–36.

1643 Villareal G, Li Q, Cai D, Fink AE, Lim T, Bougie JK, Sossin WS, Glanzman DL (2009) Role of
1644 protein kinase C in the induction and maintenance of serotonin-dependent en-
1645 hancement of the glutamate response in isolated siphon motor neurons of Aplysia
1646 californica. J Neurosci 29:5100–5107.

1647 Vonhoff F, Kuehn C, Blumenstock S, Sanyal S, Duch C (2013) Temporal coherency be-
1648 tween receptor expression, neural activity and AP-1-dependent transcription regu-
1649 lates Drosophila motoneuron dendrite development. Development 140:606–616.

1650 Walsh B, Smith A, Weber-Fox C (2006) Short-term plasticity in children's speech motor
1651 systems. Dev Psychobiol 48:660–674.

1652 Wang Y, Pillai S, Wolpaw JR, Chen XY (2006) Motor learning changes GABAergic terminals
1653 on spinal motoneurons in normal rats. Eur J Neurosci 23:141–150.

1654 Watanabe A, Kimura T, Sakaguchi H (2002) Expression of protein kinase C in song con-
1655 trol nuclei of deafened adult male Bengalese finches. Neuroreport 13:127–132.

1656 Watanabe A, Li R, Kimura T, Sakaguchi H (2006) Lesions of an avian forebrain nucleus
1657 prevent changes in protein kinase C levels associated with deafening-induced vocal
1658 plasticity in adult songbirds. Eur J Neurosci 23:2447–2457.

1659 Whitehead SC, Leone S, Lindsay T, Meiselman MR, Cowan NJ, Dickinson MH, Yapici N,
1660 Stern DL, Shirangi T, Cohen I (2022) Neuromuscular embodiment of feedback con-
1661 trol elements in flight. Sci Adv 8:eabo7461.

1662 Wieschaus E, Noell E (1986) Specificity of embryonic lethal mutations in Drosophila ana-
1663 lyzed in germ line clones. Rouxs Arch Dev Biol 195:63–73.

1664 Wolf R, Heisenberg M (1986) Visual orientation in motion-blind flies is an operant behav-
1665 iour. Nature 323:154–156.

1666 Wolf R, Heisenberg M (1991) Basic organization of operant behavior as revealed in Dro-
1667 sophila flight orientation. J Comp Physiol A 169:699–705.

1668 Wolpaw JR (2012) Harnessing neuroplasticity for clinical applications. Brain 135:e215;
1669 author reply e216.

1670 Wolpaw JR, Carp JS, Lee CL (1989) Memory traces in spinal cord produced by H-reflex
1671 conditioning: effects of post-tetanic potentiation. Neurosci Lett 103:113–119.

1672 Wolpaw JR, Lee CL (1989) Memory traces in primate spinal cord produced by operant
1673 conditioning of H-reflex. J Neurophysiol 61:563–572.

1674 Xiao L, Merullo DP, Koch TMI, Cao M, Co M, Kulkarni A, Konopka G, Roberts TF (2021) Ex-
1675 pression of FoxP2 in the basal ganglia regulates vocal motor sequences in the adult
1676 songbird. Nat Commun 12:2617.

1677 Yoshida Y, Yamada T, Sakaguchi H (2003) Activation of protein kinase C by the error sig-
1678 nal from a basal ganglia-forebrain circuit in the zebra finch song control nuclei.
1679 Neuroreport 14:645–649.

1680 Yoshihama Y, Chida K, Ohno S (2012) The KIBRA-aPKC connection: A potential regulator
1681 of membrane trafficking and cell polarity. Commun Integr Biol 5:146–151.

1682 Yoshihama Y, Sasaki K, Horikoshi Y, Suzuki A, Ohtsuka T, Hakuno F, Takahashi S-I, Ohno
1683 S, Chida K (2011) KIBRA suppresses apical exocytosis through inhibition of aPKC ki-
1684 nase activity in epithelial cells. Curr Biol 21:705–711.

1685 Zanker JM (1988) How does lateral abdomen deflection contribute to flight control
1686 ofDrosophila melanogaster? J Comp Physiol A Neuroethol Sens Neural Behav Phys-
1687 iol 162:581–588.

1688 Zha C, Sossin WS (2022) The molecular diversity of plasticity mechanisms underlying
1689 memory: An evolutionary perspective. J Neurochem 163:444–460.

1690 Zhang J, Webb DM, Podlaha O (2002) Accelerated protein evolution and origins of hu-
1691 man-specific features: Foxp2 as an example. Genetics 162:1825–1835.

1692 Zhang L, Wei X (2022) The Roles of Par3, Par6, and aPKC Polarity Proteins in Normal
1693 Neurodevelopment and in Neurodegenerative and Neuropsychiatric Disorders. J
1694 Neurosci 42:4774–4793.

1695 Zlomuzica A, Preusser F, Roberts S, Woud ML, Lester KJ, Dere E, Eley TC, Margraf J (2018)
1696 The role of KIBRA in reconstructive episodic memory. Mol Med 24:7.